Forecasting Research

Met O 11 Technical Note No. 38

The impact of satellite sounding data in the fine-mesh model

by

R.S. Bell and O.M. Hammon

December 1989

Meteorological Office (Met O 11)
London Road, Bracknell, Berkshire RG12 2SZ, England

Met O 11 Technical Note No 38

THE IMPACT OF SATELLITE SOUNDING DATA IN THE FINE-MESH MODEL

by

R. S. Bell and O. Hammon

December 1989

LONDON, METEOROLOGICAL OFFICE.
Met.O.11 Technical Note (New Series) No.38

The impact of satellite sounding data in the fine-mesh model.

06800190 551.509.313
551.507.362.2

Met O 11
Meteorological Office
London Road
Bracknell
Berkshire, England.

1. Introduction.

Satellite sounding data have long been used in numerical weather prediction. It was established from FGGE that substantial benefits can be obtained from making use of sounding data in the southern hemisphere in terms of improved forecasts (eg Uppala et. al., 1984), but it has proved much more difficult to demonstrate a beneficial impact in the northern hemisphere. One reason for this, is that there is a degree of redundancy in the observing network in the northern hemisphere . There is probably sufficient conventional data over much of the land areas and even over the ocean areas the model background is usually of quite high quality because the models are able to accurately advect information from upstream. Observations have, therefore, to be of a quality at least comparable to that of the model background before their impact is likely to be consistently positive. With regard to sounding data, this implies that we have to be particularly careful how we process and interpret the basic measurements. Sounding data is often considered within data assimilation schemes as a set of temperature profiles comparable to those derived from radiosondes, whereas, of course, the temperature profile is a highly derived product of the basic radiance measurements. This misuse of sounding data is a second reason why we have seen surprisingly little impact from their use. Work at the Meteorological Office in recent years has been directed towards ways of more directly using the radiance information (Eyre and Lorenc, 1989), taking data from the Local Area Sounding System (LASS) described by Turner et. al., (1985); and as a first stage, the retrieval was adapted to use a model forecast as background. Soundings from this forecast-background retrieval have been used since May 1988.

The case studies described in this paper have been undertaken for several reasons. Firstly, we wish to reassess LASS products in the context of data assimilation to validate the many changes (in particular the move towards a forecast-background retrieval) that have been made to the retrieval stage during the past few years. Previous assimilation studies (Bell and Hammon, 1985 and Swinbank, 1988) have not demonstrated a positive impact of LASS. All recent improvements to the retrieval stage have been justified on the basis of improved co-location statistics and not on increased forecast skill. Secondly, we wish to assess the impact of sounding data within the new Meteorological Office data assimilation system, the analysis correction scheme (Lorenc et. al., 1989), which was introduced in the fine-mesh operational model during July 1989, following a successful operational trial (Hammon et. al., 1988). Thirdly, it will enable us to see how our own LASS products compare with the latest version of the NESDIS products which, during the past year, have begun to be processed using a more physically based retrieval scheme. Fourthly, it will enable us to test a revision to the assimilation first proposed by Lorenc et al (1986), which makes allowances for the fact that in the retrieval stage, the vertical analysis of each sounding has used background information from the model and will therefore contain errors which are correlated with the background and hence with adjacent soundings. Finally, it will provide results which will act as the baseline for future runs in which the data assimilation algorithms will be tuned further to maximise the use made of sounding data.

Clearly we cannot provide a definitive assessment of the utility of sounding data in the North Atlantic on the basis of a few case studies. Such an assessment can only made by undertaking a lengthy observing system experiment along the lines of the recent OWSE-NA experiment . Before such an experiment we need to make attempts to optimise the assimilation of satellite soundings. The work described here can, therefore, be considered as preliminary to a more extensive 'real-time' parallel trial of the LASS system.

2. The cases

There are several strategies which may be adopted when choosing case studies. One can take 'interesting' operational cases, or make a choice based on an examination of the data, or choose entirely at random. Interesting operational cases tend to be those where the forecast has been poor, in which case tinkering with the analysis is almost certain to yield an improvement, or good in which case modified analyses are almost certain to degrade. Totally random choices are probably the best option if one had resources to run many cases. However, we are not in that happy position, since the number of cases must be limited in order that several alternative assimilations with different choices of data and assimilation algorithm can be run for each case. Thus, it is more profitable to concentrate on cases where the LASS data is different in some aspect from either the subjective analysis or the model background field.

Contoured and plotted 1000-500 thickness charts of LASS data are presented to the forecaster in the Central Forecast Office twice daily and these data he marks on a simple A, B, C basis:

'A' - denoting where LASS data is judged to be providing valuable input
'B' - denoting where LASS data is judged to be providing no extra information
'C' - denoting where LASS data is judged to be providing incorrect input

These scores were used as a basis for choosing cases. The majority of cases are scored 'B' and can be discounted, leaving a small selection of 'A' and 'C' cases to consider. December 1988 was chosen for the study period. The main reason for this choice is that there was only a very narrow window after NESDIS revised their retrieval system in the autumn and before NESDIS NOAA-11 soundings were introduced into operational runs (NOAA-11 has yet to be implemented in the LASS system). During December 1988, there were 7 cases marked A or C, brief comments by the forecasters were appended to the scores.

(1) pm 8th Dec : score A : LASS indicated sharper thickness trough near East Coast
(2) am 10th Dec : score C : smoother than conventional data
(3) pm 13th Dec : score A : confirmed important warming in W Atlantic
(4) am 15th Dec : score A : useful identifier of thickness trough at 20W
(5) pm 17th Dec : score C : doubts over shape of thickness contours to west of UK
(6) am 19th Dec : score A : useful for thickness troughs and ridges in N Atlantic

(7) pm 21st Dec : score C : would have expected more development in thickness trough/ridge near UK and off Newfoundland

In addition to these cases, a further case (8) was considered from 9th Aug 1989, the occasion of a particularly interesting synoptic event as the remnants of hurricane 'Dean' engaged the mid-latitude flow.

3. The choice of data

Currently LASS data is used in the operational assimilation with the following restrictions:

a) The resolution of the data is reduced by averaging, from its original resolution which is every 3rd HIRS field of view to a resolution equivalent to every 6th HIRS field of view, akin to that of NESDIS TOVS data. This is partly a cost saving measure and partly follows a worry that in the previous version of the repeated insertion assimilation scheme, a large volume of relatively dense soundings might overwhelm the impact of other data sources.

b) The data is not used over any area defined as a land point in the model. This restriction recognises the fact that historically, sounding data have proved less valuable than radiosonde data, which give an adequate land coverage in the European sector.

c) The lowest level (1000mb) is excluded, because of poor verification scores during the past few years. Co-location statistics suggest that this problem is not now apparent to the extent it once was.

d) The 3 LASS retrievals at each end of the swath are excluded, because of problems with the limb correction which have now mostly been resolved.

For this study, we used unaveraged LASS data (that is every 3rd HIRS field of view). We followed the operational practice of excluding the other data discussed in b),c) and d) above. We had intended to use the lowest level information since its presence allows the possibility of identifying retrieval problems which may contaminate other levels and it also avoids any problems in the assimilation with extrapolation of increments from higher levels, however programming problems defeated this intent.

Land data and edge of swath data were not used. Even though their quality seems now to be comparable with the remaining oceanic LASS data, their presence or absence from the system has no bearing on the assimilation impact. The validation of edge of swath data has been done using statistics, and does not require an impact study. The data over land is of little practical consequence, because the orbit characteristics mean that LASS data over land is introduced in the earlier spin-up cycles and not the main forecast cycle when a complete coverage of radiosonde data is available over Europe. Also we were much more interested in North Atlantic impact since the predominant airstream is westerly and the North Atlantic is a comparative data void .

Only data from NOAA-10 was used from either the LASS or NESDIS systems.

4. The Assimilations

Initially each case was repeated five times. Three experiments were run to compare different choices of sounding data (these are named runs A, D and E below). Two further experiments were run with some modification to the data assimilation algorithm for LASS data (named runs B and C in the subsequent text)

(A) The now operational 'analysis correction' assimilation scheme, using LASS data as discussed in the above section, within the line of sight of Lasham and NESDIS data only outside the LASS area.

(B) As (A) but using recent revisions to the observation and model error variance, including different values for clear, N*, and cloudy retrievals

(C) As (B) but including an option to constrain the assimilation such that the retrieval error is uncorrelated with the error of the background used in the retrieval process.

(D) A no-LASS experiment i.e. using NESDIS data within the LASS area

(E) A no-SAT experiment i.e. LASS and NESDIS both excluded.

In the subjective and objective assessments in the subsequent sections the no-SAT experiment is considered to be the benchmark against which the other experiments are judged.

The runs B and C are the first of several planned tuning experiments. In run A the error variance for LASS observations and model fields are the same as were used for NESDIS soundings and there was no distinction between the clear and cloudy retrievals. In run B, the error variances were taken to be the same as were used in the prior retrieval stage. These statistics had been determined from the colocation database of LASS and model background against radiosondes. Different values were used depending on the retrieval path.

In run C, the constrained assimilation involved an amplification of the original corrections made using the radiances to the background with a corresponding amplification to the estimated error. The following assumptions were made in deriving this modification to the assimilation. Firstly, we assume we have two uncorrelated estimates, the constrained retrieval $\underline{X}_a^*$ and the background $\underline{X}_b$, where the former can be determined by assuming that the minimum variance combination of $\underline{X}_a^*$ and $\underline{X}_b$ yields the original retrieval $\underline{X}_a$. Thus:

$$\underline{X}_a = \underline{X}_b + \underline{C} \cdot (\underline{C} + \underline{S}^*)^{-1} \cdot (\underline{X}_a^* - \underline{X}_b) \qquad (1)$$

where $\underline{C}$ and $\underline{S}^*$ are the error covariances for the model background and the constrained retrieval respectively. These are related to the error covariance $\underline{S}$ of the original retrieval as follows:

$$\underline{S} = \underline{C} - \underline{C} \,.\, (\underline{C} + \underline{S}^*)^{-1} \,.\, \underline{C} \qquad (2)$$

We make the assumption that that the off-diagonal terms can be ignored and thus the levels are uncoupled. For a given level, j, the above equations can be recast to determine X_a^* and S^*:

$$(X_a^* - X_b)_j = (1 + S^*/C) (X_a - X_b)_j \qquad (3)$$

$$S^* = C.S \,/\, (C - S) \qquad (4)$$

The error covariance, $\underline{S}$, of the retrieval $\underline{X}_a$ is taken from the vertical retrieval stage

$$\underline{S} = \underline{C} - (\underline{K}.\underline{C})^T (\underline{K}.\underline{C}.\underline{K}^T + \underline{E})^{-1} . \underline{K}.\underline{C} \qquad (5)$$

where $\underline{K}$ is a linear matrix of the partial derivatives of the radiative transfer equation, and $\underline{E}$ is the error covariance of the observed radiance profile.

The current values of of background error variance (C) and retrieval error variance (S) are given in table 1 below, together with the derived values of S*/C, the amplification factor for the increments. Values are given for each of three retrieval paths, at all the standard pressures on which the data is available.

Pressure (mb)	850	700	500	400	300	250	200	150	100	70	50	30
C	4.8	3.3	2.7	2.9	3.8	6.7	6.3	2.8	2.2	2.6	3.1	10.9
S-clear	3.4	1.9	1.7	2.1	3.4	5.5	5.0	2.2	1.7	1.9	2.2	8.1
S-part clear	3.8	2.2	1.8	2.2	3.4	5.4	4.7	2.1	1.6	1.9	2.2	8.1
S-cloudy	3.9	2.3	1.9	2.3	3.5	5.6	5.0	2.2	1.7	1.9	2.2	8.2
S*/C-clear	2.5	1.3	1.7	2.7	7.9	4.7	3.7	3.4	3.3	2.7	2.5	2.9
S*/C-part clear	3.8	1.9	1.9	3.1	8.4	4.2	2.9	2.7	2.9	2.8	2.5	2.9
S*/C-cloudy	4.1	2.2	2.4	3.5	9.1	5.1	3.8	3.4	3.3	3.0	2.8	3.1

Table 1- error variances C and S, and amplification factor

5. Subjective assessment

5.1 Summary

For the subjective assessment, we concentrated on the surface pressure, 500mb and 250mb height, 1000-500 thickness, 250mb winds and in forecast rainfall. The cases we shall label 1 through 8 in the chronological order as given in section 2. The five different experiments we shall label A through E as discussed in section 4.

Case	Impact of sounding data on analysis	Impact of sounding data on forecast	overall assessment
1	Deeper ridge/trough system between Norway, Greenland in C conflicts with obs -Newfoundland problem	70-80N hence minimal impact on forecast. Low 4mb deeper in A, B, C, D T+36 but fine-mesh error increased	1. E 2. A, B, D 5. C
2	Upper trough East Greenland warmed by C too much. -Newfoundland problem	Weaker trough, less rain/snow over Norway, North Sea T+24 in C Low 7mb deeper in A, B, C, D, also 250mb jet 5-10KT weaker T+24/36	1. E 2. A, B, D 5. C
3	Stronger thermal ridge in Atlantic, especially in C. 250mb jet 5-10KT stronger over Atlantic in C.	Slightly increased rain/snow associated with warm front T+24 over Norway. Anticyclone U.K 4mb higher.	1. C 2. A, B 4. D 5. E
4	-Newfoundland problem Slightly higher thickness associated with low near Greenland .	No effect on Newfoundland low which moved N during forecast. No impact on pressure of low.	minimal impact
5	No positive guidance in fixing frontal wave but slight warm bulge (1-2DM) 30-45W in C analysis.	Area of rain over U.K associated with wave slightly more accurate in C.	1. C 2. A, B, D and E
6	Small analysis differences Speed of 250mb jet 5-15 KT weaker over Eastern England at T+12 in C	Warm front weaker in C at T+18 smaller rain area forecast over over Ireland	1. A, B, D and E 5. C
7	Small analysis differences	No impact on forecasts	minimal impact
8	No help in analysis of 'Dean'. Slight warming associated with cold pool near Iceland	Negligible impact on forecast	minimal impact

Table 2. Summary of subjective assessment of the eight case studies.

Table 2 summarises the subjective assessment for all eight cases. For the most part we shall describe the results in terms of departures from (E) the NOSAT runs. Our main conclusions were that experiment C showed the greatest impact in comparison with the NOSAT benchmark runs (E). In the analyses, the largest signals were to be found in the thickness charts and in the upper winds. There was a tendency for the signal to diminish during the forecasts. No large differences were noted in any of the forecasts. The 'Newfoundland' problem alluded to in the table was of interest because the analysis differences emanated from a region to the west of the westernmost satellite orbit. In the section below we shall consider four cases in greater detail. These have been selected because they showed the greatest impact and also they contain illustrations of recurrent features. We shall not illustrate any results from experiment A in the following section because it was barely distinguishable from experiment B.

5.2 Discussion of selected cases

CASE 2. DT 12GMT 10/12/88.

a) The synoptic situation-

A 500mb ridge was the most important feature of the analysis in the eastern Atlantic, but it weakened over the U.K. during the forecast period with a westerly flow becoming established by T+36. The anticyclone centred over Biscay persisted, dominating the weather over southern Britain for most of the forecast period. However, a cold front, positioned 20-25W at T+0, moved steadily southeastwards, crossing Scotland and northern England by T+24 and reaching southern England by T+36.

b) Impact of sounding data on the 1000-500mb thickness-

NOAA 10 satellite passes at 0700 , 0840 , and 1020 GMT were used in the A,B,C and D experiments. The last two of these passes were of most interest to us, since these provided additional information over the Atlantic. The LASS data on this occasion was given only a 'C' rating by the forecasters in CFO, who considered that it smoothed out the analysis rather than adding useful data. The impact of the LASS data on the background 1000-500mb thickness is shown in Figure 1, which also illustrates the data coverage . The figures plotted show the differences in decametres between the retrieved 1000-500mb thickness from the sounding data and the fine-mesh forecast thickness . This is the fine-mesh forecast used in the retrieval and is based on 00GMT initial data , with an interpolation to the observation time. Over most of the Atlantic, differences associated with the 500mb ridge are small and the largest differences (+4 to +7DM) are seen over eastern Greenland and northern Scandinavia. In Figures 2 (i) and (ii), we compare the 1000-500mb thickness analyses following the C and E assimilation cycles. The two analyses both show the dominance of the ridge in the eastern Atlantic, but there are two main areas of difference which are hghlighted in Figure 2(iii), the C-E thickness difference chart.

The first feature is the thermal trough to the east of Greenland which is less pronounced in run C. The assimilation differences of up to 7DM in

figure 2(iii) match the plotted differences of up to 6dm in figure 1. Figure 2 (iv) shows that the thickness differences between the D and E analyses were much smaller. Surprisingly, the B analysis (not shown) was very similar to D despite having the same data as C . In the subsequent fine-mesh forecast, the analysis differences between C and E were advected eastwards with the upper trough without amplifying with time. The T+24 forecasts of the 1000-500 mb thickness from C and E are compared in figures 3 (i) and (ii). Although the two charts look very similar, C is still warmer by 2-6 dm between Greenland and Norway and this difference is highlighted in the C-E thickness difference chart, figure 3(iii).

The second feature of interest in the (C-E) thickness analysis difference chart (Figure 2 (iii)) lies in the area around Newfoundland where there is a small difference between the C and E analyses of the strong southwesterly flow south of the upper trough over Newfoundland. This area is to the west of the sounding data being used in the assimilations over the Atlantic , hence we would have expected all the analyses to have been identical over Newfoundland. All of the analyses which used the sounding data (i.e. A, B, C and D) showed the same impact. This difference occurred in a crucial position in the southwesterly jet and close to the centre of a depression on the surface at 40N 55W. In the forecast this difference was advected northwards in association with the depression increasing in magnitude from 1-3 DM at T+0 to 12DM by T+24. This difference in the forecast thickness is highlighted by the bullseye on the C-E and D-E difference charts (see Figures 3 (iii) and (iv)) just to the northeast of Newfoundland.

c) Impact of Satellite Data on forecast rain and surface pressure-

The East Greenland differences in the forecast upper air pattern between C and E did seem to have an effect on the predicted weather over Norway and the North Sea at T+24 and T+30. At T+24, 12Z 11/12/88, a complex area of low pressure extended between Iceland and Norway, with a warm front moving into southwest Norway preceded by an area of snow. The C and E mean sea level pressure and precipitation forecasts at T+24 are compared in Figures 4 (i) and (ii) respectively. The E forecast predicted a deeper centre and trough with more precipitation over Norway and the North Sea. The forecast 850mb θ_w and accumulated rain at figures 4(iii) and (iv) support these differences. Unfortunately these differences were difficult to verify due to the lack of observations in this area.

The Newfoundland difference reflects a more pronounced thermal ridge in C and B associated with the deepening depression. By T+36, the centre of the depression was 7-8mb deeper in the A, B, C and D forecasts than in the control forecast run from the E analysis. Due to an evolution error in the fine-mesh forecast of the movement of the depression, this extra deepening did not improve the forecast.

d) Impact of Satellite Data on the 250 MB winds-

Differences in the 250MB wind speed and direction developed during the forecast as a result of the analysis difference over Newfoundland. Airep reports valid around 12Z 11/12/88 suggested that the jet core across the Atlantic at 60N had a magnitude of 120-135 knots (60-70 m/s). The T+24

forecasts from the C and E analyses are compared in Figures 5 (i) and (ii). The jet core is better represented and 5-10 m/s stronger in the E forecast (if we take the airep reports as representing the truth). Both the C-E and D-E differences were similar as we can see from figures 5 (iii) and (iv). The impact of the sounding data has slightly degraded the jet forecast by smoothing out the flow. All the forecasts A, B, C and D from those analyses which used sounding data were very similar in predicting a weaker jet at 60N at T+24.

CASE 3. DT 00GMT 14/12/88.

a) The synoptic situation-

In the upper air, the major feature was the strong ridge which persisted over the western Atlantic including the British Isles throughout the forecast period, confining the baroclinic zone to the west of 30W and north of 65N. A large anticyclone controlled the weather over the British Isles throughout the forecast period with frontal systems being steered well to the north. A warm front moved eastwards into Norway after T+18, whilst in the Atlantic a cold front moved slowly eastwards.

b) Impact of Satellite Data on the 1000-500MB thickness-

NOAA-10 satellite passes at 1720, 1900, and 2040 GMT were used in the A, B, C and D assimilation cycles. The 2040GMT pass covering the western Atlantic was of most interest and the impact of the sounding data it provided on the fine-mesh background thickness is shown in Figure 6. The LASS data was given an 'A' score by the forecasters in CFO, since it confirmed the important warming in the western Atlantic. In figure 6, we see the largest LASS increments are over the western Atlantic at 35-45W (up to 8dm). The impact of the sounding data is to raise thickness values on the western side of the thermal ridge in the western Atlantic thus strengthening the thermal ridge and weakening the trough over Newfoundland. This case showed the most marked impact of all the cases of sounding data on the analysis and again, the strongest signal is seen by comparing the C and E 1000-500mb thickness analyses in Figures 7 (i) and (ii) respectively. The impact from the sounding data in the C analysis is a marked warming (1-7dm) in the analysis of the thermal ridge between 15 and 45 degrees west. This can be seen more clearly in the (C-E) difference chart at figure 7(iii), where, as in the previous case the difference in the assimilation fields is very similar to the differences in observation increments (figure 6). The thermal ridge in the C analysis is broader and extends further east. In this case , the use of sounding data was judged to have improved the thickness analysis, helping to correct a known model bias.

During the forecast , however, the difference between C and E gradually diminished. The C-E thickness difference charts shown in Figures 8 (iii) and (iv) show how the difference between the two forecasts diminished with time. At T+12, however, if we compare the C and E forecasts shown in Figures 8 (i) and (ii), we can still see a positive impact from the sounding data with the C thermal ridge extending further eastwards towards Scandinavia giving a more correct forecast. The smaller impact of the

sounding data on the B analysis is shown by the B-E thickness difference charts at T+0 and T+12 in Figures 9 (i) and (ii) respectively. The impact was much less marked and diminished quickly with time. By T+12 there was little or no difference between the B and E forecasts. A very similar result is seen from the D-E thickness charts shown by Figures 9 (iii) and (iv).

c) Impact of Satellite Data on forecast rain and surface pressure-

The intensification of the thermal ridge in C did have some impact on the forecast weather over Norway and the British Isles at T+24. This can be seen by comparing the predicted mean sea level pressure and rainfall rates at T+24 from the C and E forecasts in Figures 10 (i) and (ii) respectively. The warm front crossing Norway during the 11th was slightly more active in the C forecast, being associated with an area of higher 850MB wet-bulb potential temperature and slightly increased amounts of precipitation over the Norwegian mountains. Unfortunately, this is difficult to verify due to lack of observations. Also, the anticyclone over the U.K was slightly (4mb) stronger in the C forecast which was correct.

d) Impact of Sounding Data on the 250 MB winds-

There were little or no differences between the 250 mb analyses and forecasts from B, D and E. However in the C analysis, the Atlantic jet was analysed 5-10 KT stronger over Greenland, which was judged to be an improvement. This is illustrated in figure 11 (i) to (iii), which show C, E and C-E winds respectively

CASE 5. DT 00GMT 18/12/88.

a) The synoptic situation

An anticyclone was centred over Biscay with a strong west to northwesterly flow over the British Isles. A cold front was slow moving over the U.K.; its progress southwards being retarded by a series of waves. The main wave was centred over northwest England at T+24.

b) Impact of sounding data on the 1000-500MB thickness-

NOAA-10 satellite passes at 1600, 1730, 1910 and 2100 GMT were used in the A, B, C and D assimilation cycles. The coverage of sounding data over the Atlantic is shown in Figure 12. The 1910 and 2100GMT passes were potentially of most use to help in the analysis of minor troughs and ridges in the Atlantic which could perhaps be associated with a developing wave on the cold front. However, the LASS data was given a 'C' score by the forecasters in CFO, since they did not find the data helpful. The plotted differences in decametres between the retrieved 1000-500mb thickness from the sounding data and the fine-mesh T+6 forecast background thickness in figure 12 show that the main impact of the sounding data was near the western edge of the swathe at 45-55N, 40-50W, with small positive increments (2-4dm) in the southwesterly jet. However the differences were too small to give any positive guidance in fixing the position of a wave on the cold front in this area.

The small impact of sounding data in the Atlantic in the C analysis is shown in the C-E 1000-500mb thickness difference chart in figure 13 (iii). Comparing the C and E analyses in figures 13 (i) and (ii) we see that the difference results from a less sharp thermal trough in the C run south of Greenland with perhaps just a hint of a warm bulge to the south of the strong thermal gradient, indicative of a wave on the cold front. Figure 13(iv) shows the small differences between the C and E thickness forecasts at T+24.

c) Impact of sounding data on forecast rain and surface pressure-

The small positive differences in the western Atlantic in the C analysis have been advected eastwards to be over the U.K at T+24 in association with a wave on the cold front. There was a consequential improvement in the forecast rain area over the U.K at T+24. The observed rain area over Scotland and northern England at 00GMT 19/12/88, associated with the wave over the U.K is shown in Figure 14 (iii). This area may be compared with the T+24 forecast rain areas from the C forecast (Figure 14(i)) and the E forecast (Figure 14(ii)). Although both forecasts have predicted the area of rain too far south, the C forecast is more accurate.

In the B and D analyses, there was very little impact from the sounding data.

CASE 6. DT 12GMT 19/12/88.

a) The synoptic situation-

A frontal system in the Atlantic moved eastwards with the warm front crossing the U.K. on the 20th and the cold front becoming slow moving over southern Scotland by T+36. However, the main feature of interest was the strength of the polar jet across the Atlantic with maximum reported wind speeds at 250MB of 150-180 knots (75-90 metres per second).

b) Impact of Satellite Data on the 1000-500MB thickness-

NOAA-10 satellite passes at 0840 GMT and 1020 GMT were used in the A, B, C and D assimilation cycles. The LASS data was given an 'A' score by the forecasters in CFO, since they found the data useful in the analysis of thickness troughs and ridges in the North Atlantic. However the sounding data had only a small impact on the A, B, C and D analyses on the western side of the upper ridge at 60N 40W. These differences were advected northeastwards in the forecasts to the north of 70N, hence the impact on the forecast was negligible.

c) Impact of Satellite Data on the 250 MB wind-

The 250mb wind analyses following the C and E assimilation cycles were very similar, as shown by Figures 15 (i) and (ii). Both have a good analysis of the speed of the jet across the Atlantic and few areas of difference show up in figure 15(iii) for (C-E) . However, in the C forecast, small differences developed at T+06 onwards which affected the predicted wind speed of the warm front jet over the U.K. Figure 16 (iv) shows the

observed 250mb winds for 00GMT 20/12/88, with maximum speeds between 145 and 165 knots (72-82 metres per second). Both C and E forecasts for T+12 predicted the position and strength of the mid-Atlantic SW jet accurately. These forecasts can be compared in Figures 16 (i) and (ii). The difference chart, Figure 16(iii) shows that the C wind speed forecast is 10-30 knots (5-15 metres per second) lighter in the core of the jet over Eastern England (i.e. max speed 164KT instead of 176KT).

c) Impact of Satellite Data on forecast rain-

Although the difference between the jets was small, there was some impact on the intensity of the rain area associated with the warm front as it crossed Ireland. By 06GMT 20/12/88, Figure 17(iii) shows that the rain area had already spread across Ireland into Cornwall, west Wales and west Scotland. This observed weather can be compared with the T+18 rain rate forecasts from the C and E forecasts shown in Figures 17 (i) and (ii) respectively. Both are slow with the timing of the rain but the warm front is noticeably weaker in the C forecast and the E forecast is more accurate. The forecasts from the B and D analyses were much more like the E forecast.

6. Objective assessment

Forecasts were verified over the whole fine-mesh area using radiosondes and surface reports. In table 3 below, rms errors for the T+12 forecasts are given as averages from eight cases. The actual values are given for the NO-SAT runs (E). For the other runs, the values are expressed as a percentage of the NO-SAT run.

	E	A	B	C	D
Surface Pressure (mb)	2.5	100	100	109	100
850mb Height (dm)	1.7	101	101	114	100
700mb Height (dm)	1.9	100	100	108	100
500mb Height (dm)	2.5	98	98	102	100
250mb Height (dm)	3.5	99	99	99	101
850mb Temperature (degC)	2.0	99	99	102	101
700mb Temperature (degC)	1.7	96	96	97	100
500mb Temperature (degC)	1.5	99	99	101	103
250mb Temperature (degC)	2.0	99	98	103	104
850mb Vector Wind (m/s)	5.5	100	100	101	101
700mb Vector Wind (m/s)	5.1	100	100	101	101
500mb Vector Wind (m/s)	5.9	99	99	100	100
250mb Vector Wind (m/s)	8.2	101	101	100	100
850mb RH (%)	20.9	99	99	99	100
700mb RH (%)	23.3	100	100	102	101
500mb RH (%)	26.8	100	100	101	100
mean for all variables=		99.4	99.3	102.4	100.7

Table 3 - T+12 verification against observations with values for runs A-D expressed as % of 'E' runs

In table 3, we see relatively small differences between the various experiments. The LASS-A and LASS-B runs verified marginally better than NO-SAT, whilst the NESDIS run (D) verified marginally worse. The 'constrained assimilation' LASS-C run was particularly poor for surface pressure and the lowest level height fields.

As the forecasts proceded, the relative accuracy of the runs changed, as we can see from tables 4 and 5 below which give the same information as for table 3 but for the later forecast periods, T+24 and T+36 respectively. There is little impact from our revision of the assumed background and observation errors (LASS-A compared with LASS-B). At T+24, the height fields are better for LASS-B compared with the NO-SAT run, but the upper winds are slightly worse. The LASS-C run is now best, mainly because of improved height fields, whilst the NESDIS run is giving the worst scores. By T+36, runs LASS-A, LASS-B and NESDIS are all worse than NO-SAT, with the largest departure from the NO-SAT scores being 3% at 850mb heights (representing a degradation in rms error of 0.8metres) and the same at 250 mb winds (which is 0.3m/s increase in rms error). LASS-C is comparable to NO-SAT, with the degradation in the wind fields being balanced by an improvement in height fields.

	E	A	B	C	D
Surface Pressure (mb)	3.2	100	100	99	101
850mb Height (dm)	2.2	100	100	98	101
700mb Height (dm)	2.6	98	98	96	98
500mb Height (dm)	3.5	97	97	94	100
250mb Height (dm)	4.8	98	97	94	101
850mb Temperature (degC)	2.2	100	100	100	100
700mb Temperature (degC)	2.0	97	97	98	101
500mb Temperature (degC)	2.1	100	100	100	103
250mb Temperature (degC)	2.2	100	101	102	102
850mb Vector Wind (m/s)	5.9	100	100	101	101
700mb Vector Wind (m/s)	5.8	101	100	102	100
500mb Vector Wind (m/s)	7.3	100	100	100	100
250mb Vector Wind (m/s)	9.8	102	102	101	101
850mb RH (%)	21.4	99	99	100	101
700mb RH (%)	25.1	100	100	101	102
500mb RH (%)	28.5	101	100	101	99
mean for all variables=		99.6	99.4	99.2	100.7

Table 4 - as table 3 but for T+24

	E	A	B	C	D
Surface Pressure (mb)	4.3	102	102	98	102
850mb Height (dm)	2.9	103	103	100	103
700mb Height (dm)	3.2	102	102	99	102
500mb Height (dm)	4.2	101	101	98	102
250mb Height (dm)	5.4	101	101	99	103
850mb Temperature (degC)	2.7	100	100	102	100
700mb Temperature (degC)	2.2	99	99	99	101
500mb Temperature (degC)	2.2	101	101	100	102
250mb Temperature (degC)	2.7	101	101	101	101
850mb Vector Wind (m/s)	6.8	101	100	101	101
700mb Vector Wind (m/s)	6.7	101	101	101	101
500mb Vector Wind (m/s)	8.6	102	102	101	102
250mb Vector Wind (m/s)	11.3	103	103	103	102
850mb RH (%)	25.2	100	100	99	100
700mb RH (%)	28.9	99	99	100	100
500mb RH (%)	31.3	100	100	99	99
mean for all variables=		101.0	100.9	100.0	101.3

Table 5 - as table 3 but for T+36

The same objective scores are presented in an alternative way in tables 6-8, with each set of runs being compared with another set of runs and the number of cases of a lower rms error noted. Six pairs have been considered as indicated in the key below. Run A has been excluded from this comparison because of its similarity with run B. The bolder figures in

these tables highlight case count victories by a margin of better than 5/3 where we might attach more significance to the result.

The KEY for tables 6-8 is as follows:
B/E : LASS B versus NO SAT
C/E : LASS C versus NO SAT
D/E : NESDIS versus NO SAT
B/C : LASS B versus LASS C
B/D : LASS B versus NESDIS
C/D : LASS C versus NESDIS

	B/E	C/E	D/E	B/C	B/D	C/D
Surface Pressure	4 /4	2 /**6**	4 /4	**6½**/1½	4 /4	2 /**6**
850mb Height	3½/4½	1 /**7**	4 /4	**7** /1	3½/4½	1½/**6½**
700mb Height	4 /4	2 /**6**	4 /4	**6½**/1½	4 /4	2 /**6**
500mb Height	5 /3	3 /5	3½/4½	**6** /2	**5½**/2½	3½/4½
250mb Height	5 /3	**6** /2	2½/**5½**	3½/4½	**5½**/2½	**6** /2
850mb Temperature	4½/3½	2½/**5½**	3½/4½	**6** /2	5 /3	3 /5
700mb Temperature	**6½**/1½	**6** /2	4 /4	4½/3½	**6½**/1½	**6** /2
500mb Temperature	4½/3½	3½/4½	2½/**5½**	5 /3	**6** /2	4 /4
250mb Temperature	**5½**/2½	1½/**6½**	1 /**7**	**7½**/0½	**7** /1	5 /3
850mb Vector Wind	4 /4	2 /**6**	2 /**6**	**7** /1	**6½**/1½	3 /5
700mb Vector Wind	5 /3	2½/**5½**	2 /**6**	**7½**/0½	**6** /2	3 /5
500mb Vector Wind	**6½**/1½	3½/4½	4½/3½	**7** /1	**5½**/2½	3½/4½
250mb Vector Wind	3½/4½	4 /4	4 /4	3½/4½	3½/4½	4½/3½
850mb RH	4 /4	**5½**/2½	4½/3½	3 /5	4½/3½	4½/3½
700mb RH	4½/3½	2 /**6**	3 /5	5 /3	**5½**/2½	5 /3
500mb RH	3 /5	3½/4½	5 /3	**6** /2	4 /4	3½/4½
TOTAL	73/55	50½/77½	54/74	91½/36½	82½/45½	60/68

Table 6 - case count for T+12 ; taking pairs of cases and scoring 1 for a lower rms error

On this measure we see from table 6, that the LASS-B runs win by a substantial margin at T+12. The NO-SAT runs are comfortably beating the LASS-C runs and the NESDIS runs. The LASS-C runs did score well for several fields but a very poor performance at the surface and low level height fields pushed the total score in favour of NO-SAT in the C/E comparison and also in favour of NESDIS in the C/D comparison.

At T+24, we see from table 7 below, that LASS-B and LASS-C are performing equally well and both are beating NESDIS and NO-SAT comfortably. The NESDIS runs are trailing some way behind NO-SAT in last place. By T+36 (table 8), the NESDIS runs remain firmly in last place, although there is an indication that they are not performing as badly as the LASS runs for 250mb winds. The LASS-B runs are now outperformed by the NO-SAT runs mainly because of poorer wind scores. LASS-C runs remain better overall than NO-SAT despite a poor performance at 250mb winds.

	B/E	C/E	D/E	B/C	B/D	C/D
Surface Pressure	3½/4½	3½/4½	3½/4½	3½/4½	4 /4	5/3
850mb Height	4½/3½	5 /3	4 /4	3½/4½	4½/3½	**5½**/2½
700mb Height	4 /4	5 /3	5 /3	3 /5	4 /4	**5½**/2½
500mb Height	**6** /2	**6** /2	5 /3	2 /**6**	**6½**/1½	**6** /2
250mb Height	**6½**/1½	**8** /0	2½/**5½**	1½/**6½**	**8** /0	**8** /0
850mb Temperature	3½/4½	4 /4	4 /4	3½/4½	3½/4½	4 /4
700mb Temperature	**6** /2	**6** /2	4½/3½	4½/3½	**6½**/1½	**6** /2
500mb Temperature	4 /4	4½/3½	2½/**5½**	4 /4	5 /3	5 /3
250mb Temperature	3 /5	3½/4½	3 /5	4 /4	5 /3	4½/3½
850mb Vector Wind	3½/4½	5 /3	2½/**5½**	4 /4	**6** /2	5 /3
700mb Vector Wind	4½/3½	1½/**6½**	3 /5	**6½**/1½	4 /4	2½/**5½**
500mb Vector Wind	**6** /2	4 /4	5 /3	**5½**/2½	5 /3	3 /5
250mb Vector Wind	4 /4	5 /3	3½/4½	2½/**5½**	2½/**5½**	4½/3½
850mb RH	4½/3½	5 /3	1½/**6½**	4 /4	**7½**/0½	4 /4
700mb RH	4 /4	1½/**6½**	4 /4	**6** /2	5 /3	3½/4½
500mb RH	3 /5	3½/4½	4 /4	**6** /2	3 /5	2 /**6**
TOTAL	70½/57½	71/57	57½/70½	64/64	80/48	74/54

Table 7 - as for table 6 but for T+24

	B/E	C/E	D/E	B/C	B/D	C/D
Surface Pressure	4 /4	5 /3	3½/4½	1½/**6½**	4 /4	**7** /1
850mb Height	2½/**5½**	4½/3½	2½/**5½**	2½/**5½**	5 /3	**5½**/2½
700mb Height	4 /4	4½/3½	4½/3½	3 /5	4 /4	4½/3½
500mb Height	5 /3	**5½**/2½	5 /3	3 /5	4½/3½	**5½**/2½
250mb Height	3½/4½	4 /4	3 /5	3 /5	**6½**/1½	**6** /2
850mb Temperature	3½/4½	2½/**5½**	4 /4	5 /3	3½/4½	4 /4
700mb Temperature	5 /3	4½/3½	3½/4½	4 /4	**5½**/2½	5 /3
500mb Temperature	3½/4½	4 /4	3 /5	3 /5	4½/3½	4 /4
250mb Temperature	4½/3½	5 /3	3½/4½	5 /3	**5½**/2½	**5½**/2½
850mb Vector Wind	3½/4½	4½/3½	3½/4½	3½/4½	5 /3	4½/3½
700mb Vector Wind	3½/4½	4 /4	2½/**5½**	3 /5	4½/3½	**6** /2
500mb Vector Wind	3 /5	4 /4	3 /5	4 /4	5 /3	5 /3
250mb Vector Wind	1 /**7**	2 /**6**	2 /**6**	3½/4½	2 /**6**	3 /5
850mb RH	4 /4	4 /4	3 /5	3 /5	4½/3½	5 /3
700mb RH	**5½**/2½	5 /3	5 /3	**5½**/2½	**6** /2	4 /4
500mb RH	4½/3½	**6** /2	5 /3	3 /5	1½/**6½**	3½/4½
TOTAL	60½/67½	69/59	56½/71½	55½/72½	71½/56½	78/50

Table 8 - as for table 6 but for T+36

The final table (9) gives an objective verification of the forecast 1000-500 thickness fields. Verification against observations was unavailable for this field so we must rely on a comparision with verifying analyses. The area verified is enclosed by 75N, 35N, 70W and 30E. The format is as in the above tables. It is doubtful how much we confidence we can place on these results for the shortest forecast period because the

verifying fields would contain LASS data albeit at degraded resolution and there might be a positive correlation with the LASS forecast runs. We do see an improving trend for LASS-C as the forecast progresses.

	B/E	C/E	D/E	B/C	B/D	C/D
T+12	**6**/2	3/5	3½/4½	**6**/2	**7**/1	4/4
T+24	5/3	4/4	3½/4½	**6**/2	**6**/2	3/5
T+36	5/3	5/3	4 /4	3/5	5/3	5/3

Table 9 - case count for 1000-500 mb thickness ; taking pairs of cases and scoring 1 for a lower rms error

7. Conclusions and suggestions for future work

The overall conclusions from the subjective assessment of the benefit of the use of sounding data in fine-mesh forecasts in these eight cases was inconclusive, with the NO-SAT forecast being clearly worse in only one case. The main points are listed below:

i) In general, the impact of the sounding data on the eight cases studied was small with no major change in forecast evolution. Nevertheless, we have shown that small differences, particularly in the predicted strength of the jet, can cause differences in forecast rainfall intensity and amount (cases 3 and 6).

ii) In the Newfoundland problem, small analysis differences west of the satellite swath in the baroclinic zone increased during the forecast in three cases . In two of the cases (1 and 2) a developing depression deepened more in the forecasts which used the sounding data. Due to evolution problems in the forecast, the increased deepening did not verify well. This suggests that we should make some attempt to tune the influence area for LASS data to avoid the situation where a large amount of data some distance upstream can negate the impact of isolated radiosonde reports. The problem is perhaps exacerbated in this instance because Newfoundland is on the edge of the fine-mesh domain and there is a one-sided distribution of observations.

iii) The lack of impact of sounding data in the LASS-A and LASS-B assimilations was disappointing. Even when there were large differences between the sounding data and the background, these runs seemed to smooth out the differences so that the analysis differences were small and diminished quickly with time in the forecast. One possible reason for the analysis differences reducing rather than growing with time during the forecast, is that the data was possibly correcting a large scale bias in the temperature field which occurs because the model is too slow to warm up an airmass leaving a cold continent and moving over a warm sea. In the runs without sounding data the warming still occurred without the help of observations, but on a longer timescale, so that by T+24 the SAT and NO-SAT runs were more similar than at T+0.

iv) LASS-C analysed the soundings closely (as evidenced by the match between [observation-background] increments and [LASS-C - NO-SAT] analyses) so that the greatest impact was always seen with these runs. In the subjective forecast assessment , LASS-C forecasts improved on the rest in two of the eight cases (3 and 5) but was worse in three cases (1, 2 and 6). However, two of the poorer cases (1 and 2) were caused by the Newfoundland problem.

v) No benefits were noticed from the use of NESDIS.

We have seen in section 6, that the objective verification confirmed the subjective assessment. In summary the objective results demonstrated that:

vi) The closer fit to the soundings in LASS-C was clearly detrimental to the surface pressure and low level height fields in the early stages of the forecast but the improvements in UK weather noted in the later stages were confirmed by improved verification against radiosondes. (The problem to the east of Newfoundland would not affect the objective scores). The poor fit to surface pressure at T+12 is possibly related to an increase in noise (as measured by rms pressure tendency) exhibited in some, but not all, LASS-C runs relative to LASS-B runs. This might indicate that we were forcing in increments from erroneous soundings which had not been correctly identified by quality control.

vii) LASS-A and LASS-B were marginally better than the NO-SAT run at first, but worsened towards the end of the forecast. This was disappointing, particularly as the fields contributing most to the overall deterioration were the more important surface pressure and upper wind fields.

viii) LASS runs were an improvement on the NESDIS runs which were worse than NO-SAT at all forecast periods.

We intend to pursue alternative formulations of the vertical processing within the assimilation, including the use of vertical filters to effectively degrade the vertical resolution and the interpretation of the data more properly as layer thickness by calculating model thickness increments at observation points. The improved use of geostrophic increments, particularly at higher levels, will also be considered in an attempt to improve on the upper wind verification . It is possible that with a data source of such uniform high data density the large horizontal sphere of influence in the current scheme is unnecessary, so iterating sounding data separately from other data with a reduced sphere of influence is another option to be considered. Although these changes may be very beneficial they are unlikely to be relevant to a LASS/NESDIS comparison because the changes could apply equally to both data sources.

It was not possible to demonstrate that features which the intervention forecasters identified in the data could be followed in the subsequent forecasts. It has been established (Ballard, pers comm) that some of the features were clearly the result of incorrect quality control decisions in the early stages of the retrieval process. This erroneous data might well have had a negative impact on the forecasts. Improvements in the preprocessing prior to the assimilation seem to be required.

References

Bell R S and O Hammon 1985 The impact of data from the HERMES system on the fine-mesh data assimilation scheme- a case study, Met O 11 Technical Note No 199

Eyre J and A Lorenc 1989 Direct use of satellite radiances in numerical weather prediction. Meteorol Mag **118** , 13-16.

Hammon O, R Bromley and B Macpherson	1989	The trial of the fine-mesh version of the analysis correction scheme. Met O 11 Technical Note No 26
Lorenc A, W Adams and J Eyre	1986	The analysis of high resolution satellite data in the Meteorological Office. Workshop Proc. High Res Analysis, ECMWF
Lorenc A, R S Bell and B Macpherson	1989	The new Meteorological Office data assimilation scheme, Met O 11 Technical Note No 27
Swinbank R	1988	Assessment of HERMES soundings processed using the new cloud clearing scheme, Met O 11 Technical Note No 6
Turner J, J Eyre D Jerrett and E McCallum	1985	The HERMES System, Meteorol Mag **114**, 161-173
Uppala S, A Hollingsworth, S Tibaldi and P Kallberg	1984	Results from two recent observing system experiments at ECMWF. Workshop Proc. Data assim. sys. and obs. sys. expts. for FGGE, ECMWF

Figures

Figure 1 Thickness difference between the retrieved 1000-500mb thickness from sounding data from NOAA-10 passes at 0700Z, 0840Z and 1020Z 10/12/88 and the fine-mesh forecast background thickness.

Figure 2 (i) Fine-mesh C 1000-500mb thickness analysis at 12Z 10/12/88
(ii) As (i) but for E
(iii) C-E 1000-500mb thickness analysis difference chart 12Z 10/12/88
(iv) As (iii) but for D-E

Figure 3 (i) Fine-mesh C 1000-500mb thickness forecast at T+24, valid 12Z 11/12/88
(ii) As (i) but for E
(iii) C-E 1000-500mb forecast thickness difference chart for T+24, valid 12Z 11/12/88
(iv) As (iii) but for D-E

Figure 4 (i) Fine-mesh C T+24 forecast pmsl and rainfall rates valid 12Z 11/12/88
(ii) As (i) but for E

Figure 5 (i) Fine-mesh C 250mb wind forecast at T+24 valid 12Z 11/12/88
(ii) As (i) but for E
(iii) Fine-mesh C-E 250MB wind speed differences at T+24
(iv) As (iii) but for D-E

Figure 6 Thickness difference between the retrieved 1000-500mb thickness from sounding data from NOAA-10 passes at 1720Z, 1900Z and 2040Z 13/12/88 and the fine-mesh forecast background thickness.

Figure 7 (i) Fine-mesh C 1000-500mb thickness analysis at 00Z 14/12/88

(ii) As (i) but for E

(iii) C-E 1000-500mb thickness analysis difference chart 00Z 14/12/88

Figure 8 (i) Fine-mesh C T+12 1000-500mb thickness forecast for 12Z 14/12/88

(ii) As (i) but for E

(iii) C-E T+12 1000-500mb thickness forecast difference chart 12Z 14/12/88

(iv) As (iii) but for D-E

Figure 9 (i) B-E 1000-500mb thickness analysis difference chart 00Z 14/12/88

(ii) B-E T+12 forecast thickness difference chart valid 12Z 14/12/88

(iii) As (i) but for D-E

(iv) As (ii) but for D-E

Figure 10(i) C T+24 fine-mesh forecast of rainfall rate and mean sea level pressure valid 00Z 15/12/88

(ii) As (i) but forecast E

Figure 11(i) Fine-mesh C 250mb wind analysis valid 00Z 14/12/88

(ii) As (i) but for E

(iii) Fine-mesh C-E 250MB wind speed analysis differences

Figure 12 Thickness difference between the retrieved 1000-500mb thickness from sounding data from NOAA-10 passes at 1600Z, 1730Z, 1910Z and 2100Z 17/12/88 and the fine-mesh forecast background thickness.

Figure 13(i) Fine-mesh C 1000-500mb thickness analysis at 00Z 18/12/88

(ii) As (i) but for E

(iii) C-E 1000-500mb thickness analysis difference chart 00Z 18/12/88

(iv) C-E 1000-500mb forecast thickness difference chart for T+24, valid 00Z 19/12/88

Figure 14(i) Fine-mesh model C T+24 forecast of rainfall rate and mean sea level pressure valid 00Z 19/12/88

(ii) As (i) but forecast E

(iii) Observed rain area at 00Z 19/12/88

Figure 15(i) Fine-mesh C 250mb wind analysis valid 12Z 19/12/88

(ii) As (i) but for E

(iii) Fine-mesh C-E 250MB wind speed analysis differences valid 12Z 19/12/88

Figure 16(i) Fine-mesh C 250mb wind forecast at T+12 valid 12Z 20/12/88

(ii) As (i) but for E

(iii) Fine-mesh C-E 250MB wind speed differences at T+12

(iv) Observed 250mb winds for 00Z 20/12/88

Figure 17(i) Fine-mesh model C T+18 forecast of rainfall rate and mean sea level pressure associated with warm front valid 06Z 20/12/88

(ii) As (i) but forecast E

(iii) Observed rain area at 06Z 20/12/88 associated with warm front

FIGURE 1. THICKNESS DIFFERENCE BETWEEN THE RETRIEVED 1000-500MB THICKNESS FROM SOUNDING DATA AND THE FINE-MESH FORECAST BACKGROUND THICKNESS

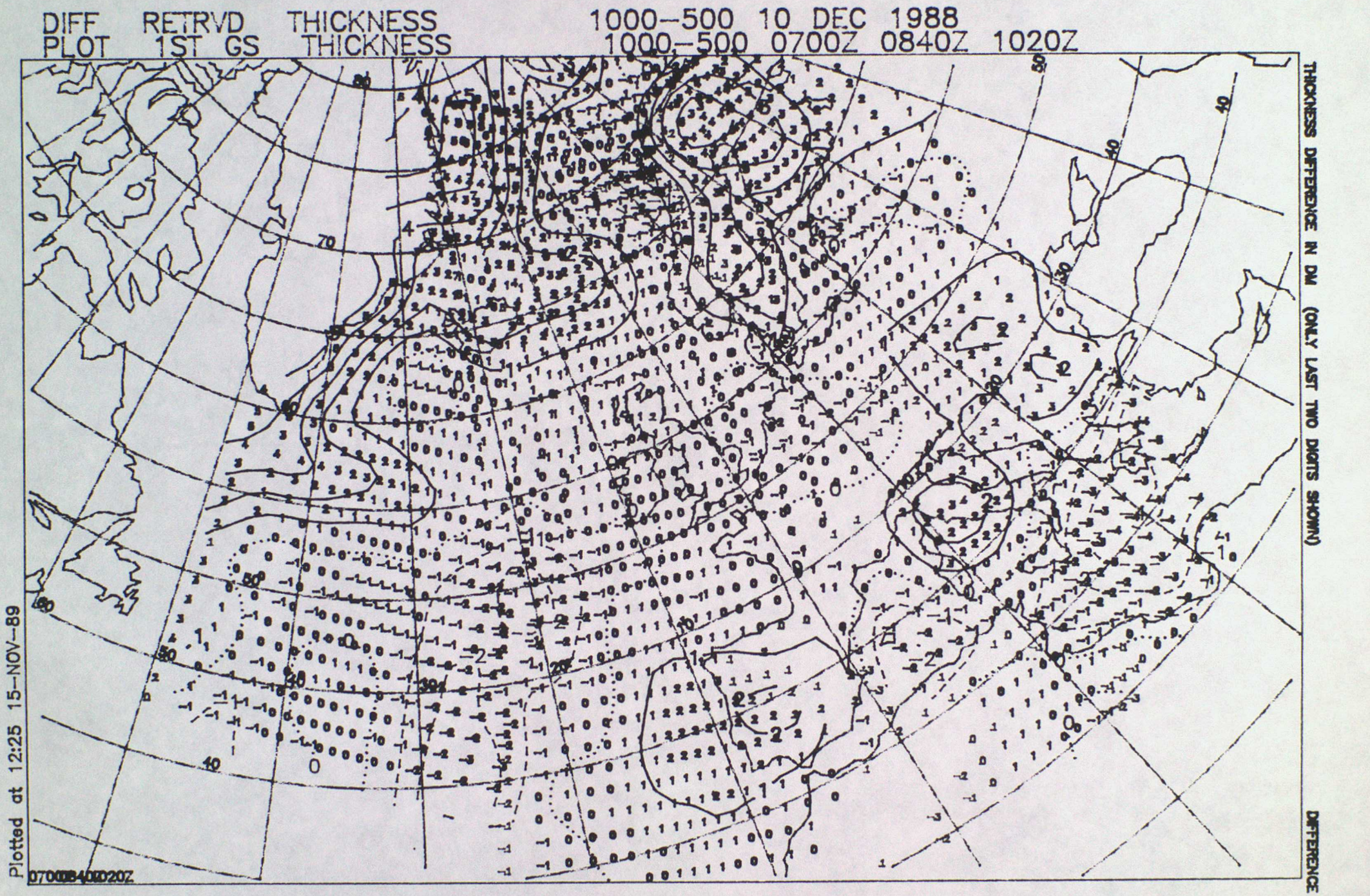

(i) FOLLOWING THE C ASSIMILATIONS

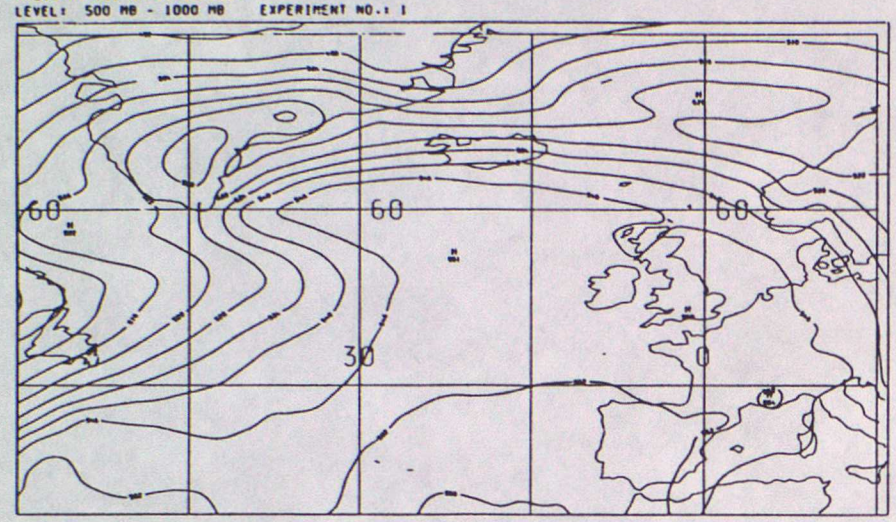

(ii)FOLLOWING THE E ASSIMILATIONS

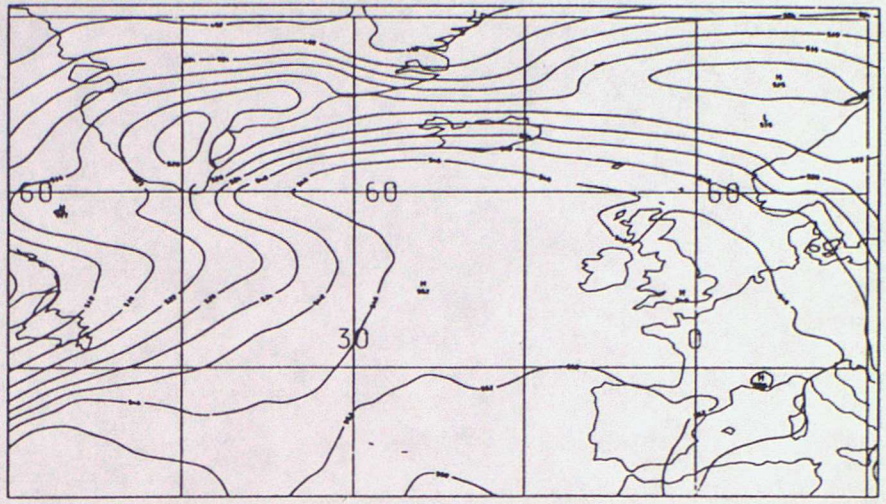

FIGURE 2. FINE-MESH 1000-500MB THICKNESS DIFFERENCE CHARTS VALID 12Z 10/12/88

(iii) C-E

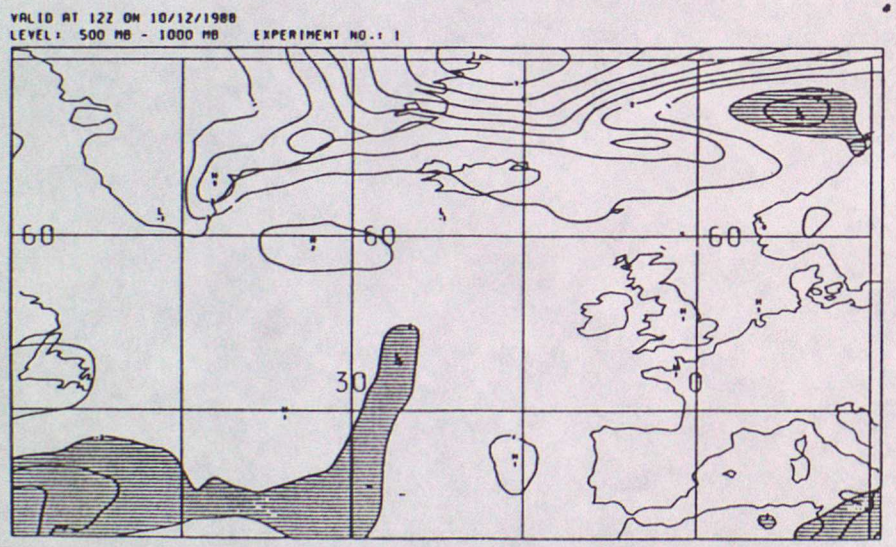

(iv) D-E

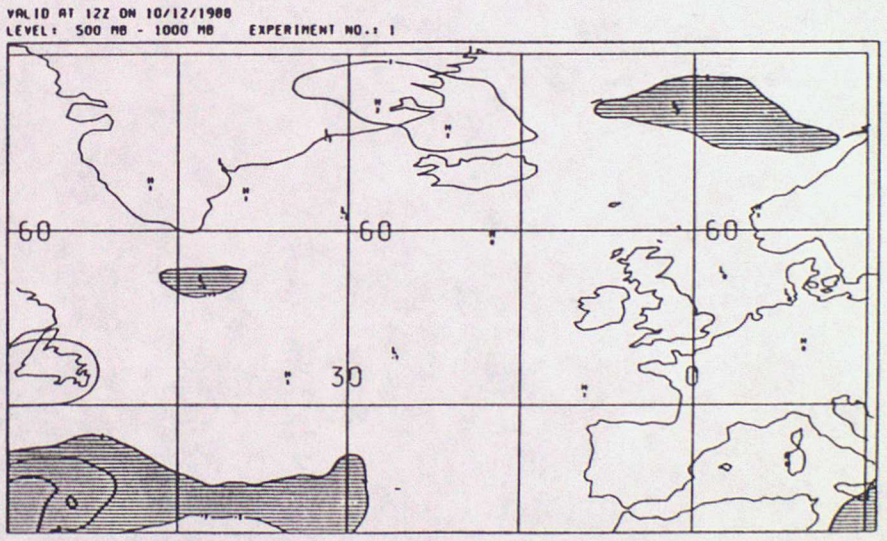

FIGURE 3. FINE-MESH 1000-500MB THICKNESS FORECAST AT T+24 VALID 12Z 11/12/88

(i) EXPERIMENT C

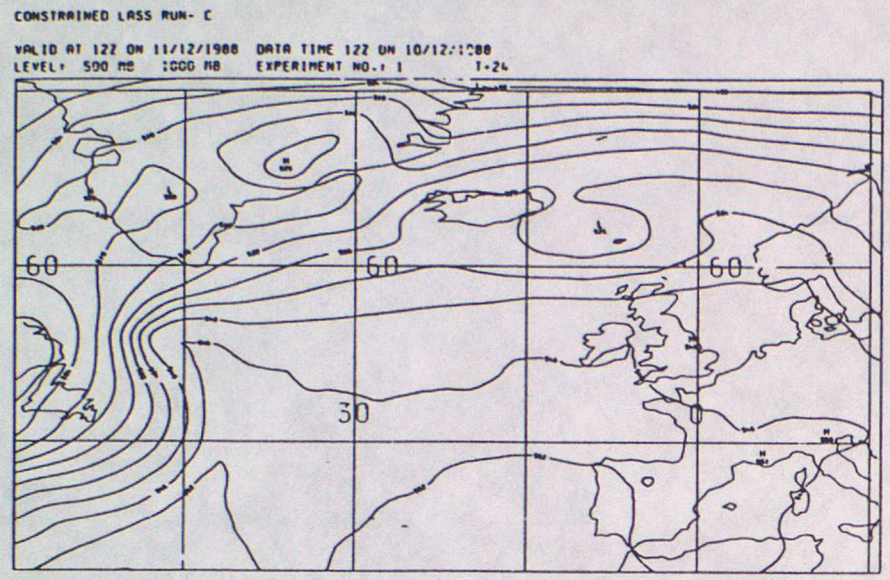

(ii)EXPERIMENT E

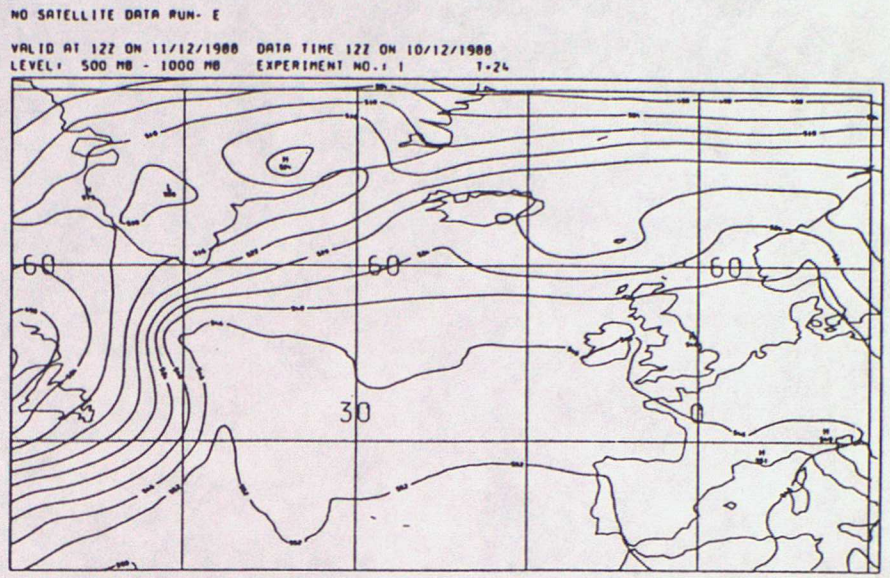

FIGURE 3. FINE-MESH 1000-500MB FORECAST THICKNESS DIFFERENCE CHARTS AT T+24 VALID 12Z 11/12/88

(iii) C-E

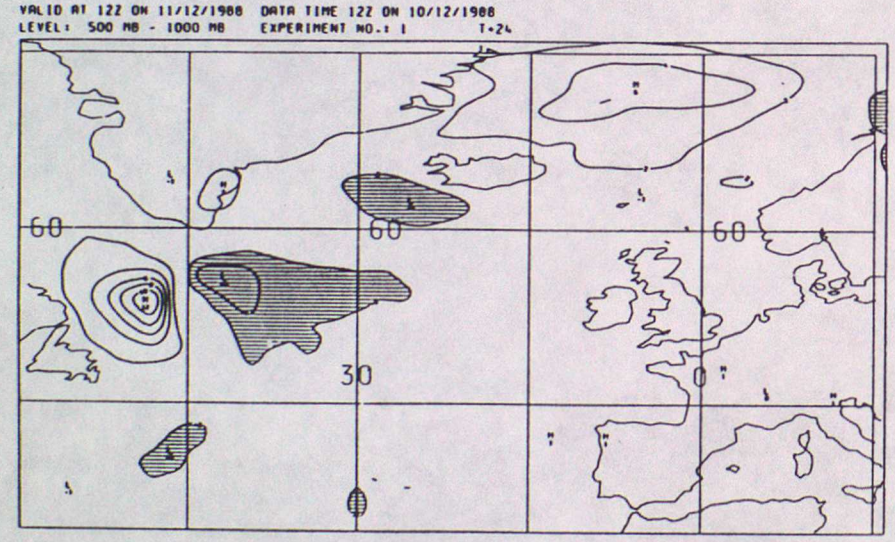

(iv) D-E

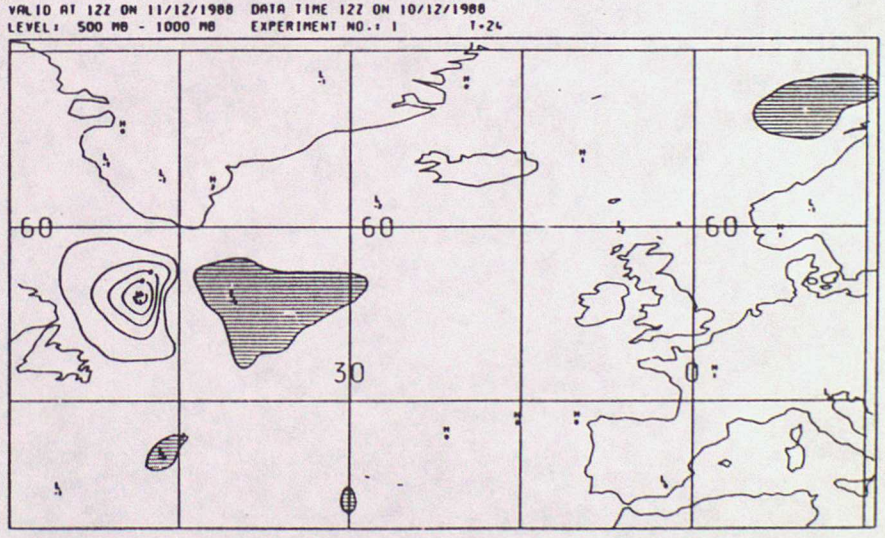

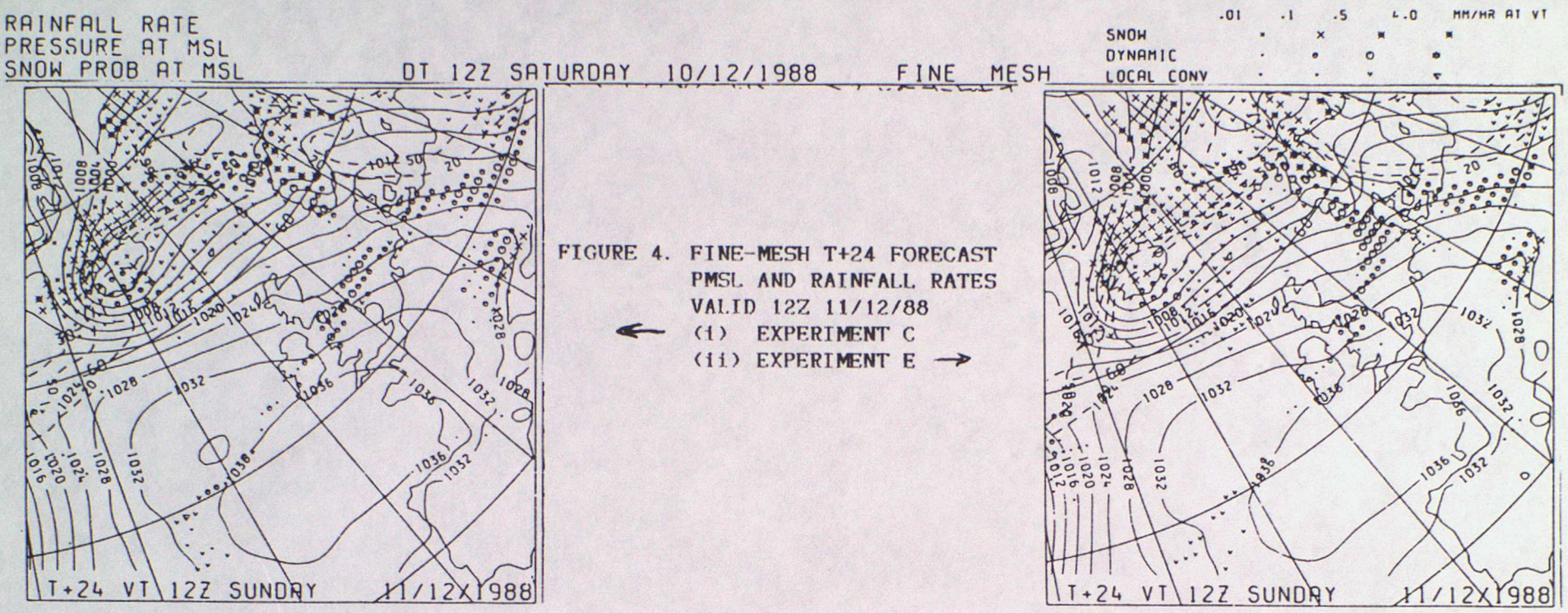

FIGURE 4. FINE-MESH T+24 FORECAST
PMSL AND RAINFALL RATES
VALID 12Z 11/12/88
(i) EXPERIMENT C ←
(ii) EXPERIMENT E →

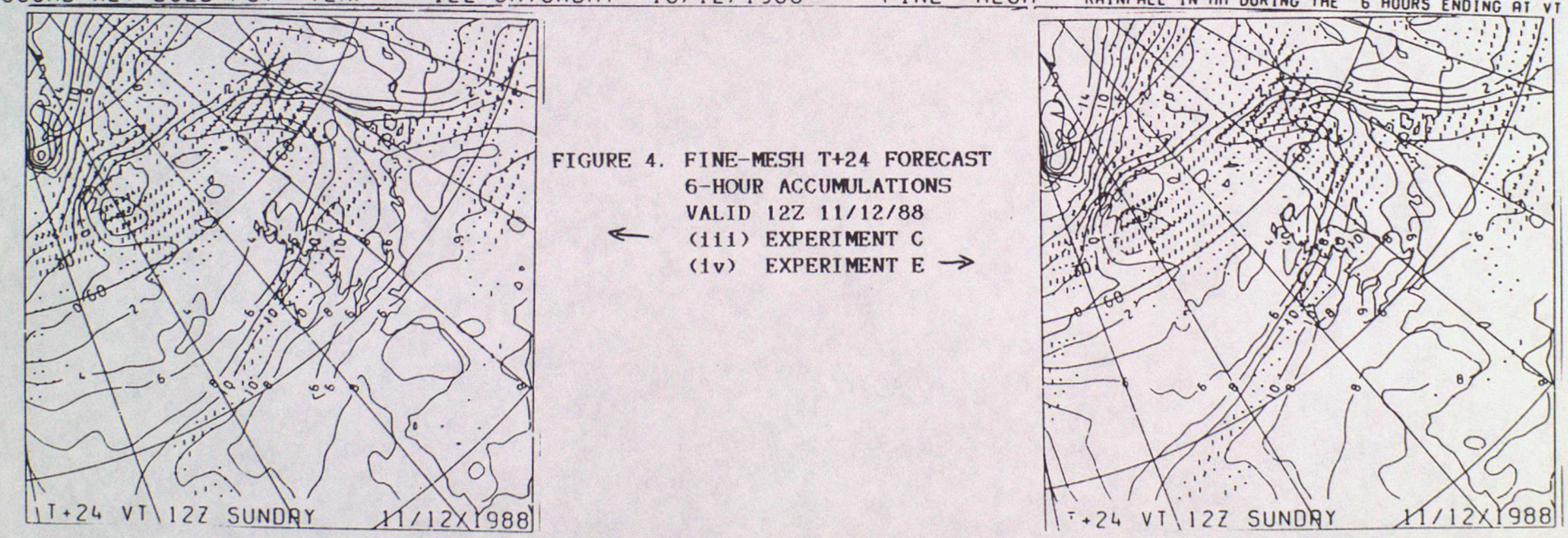

FIGURE 4. FINE-MESH T+24 FORECAST
6-HOUR ACCUMULATIONS
VALID 12Z 11/12/88
(iii) EXPERIMENT C ←
(iv) EXPERIMENT E →

FIGURE 5. FINE-MESH 250MB WIND FORECAST AT T+24 VALID 12Z 11/12/88

(i) EXPERIMENT C

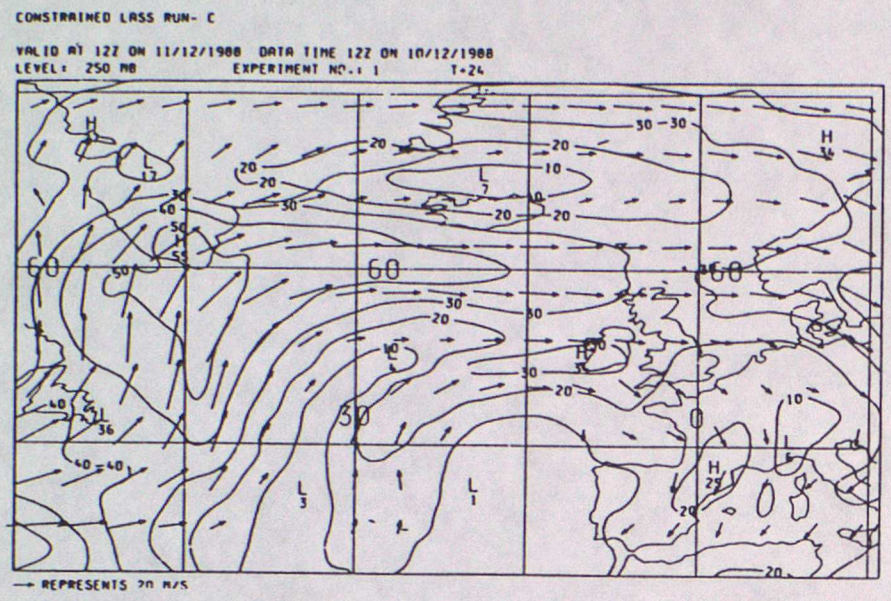

(ii) EXPERIMENT E

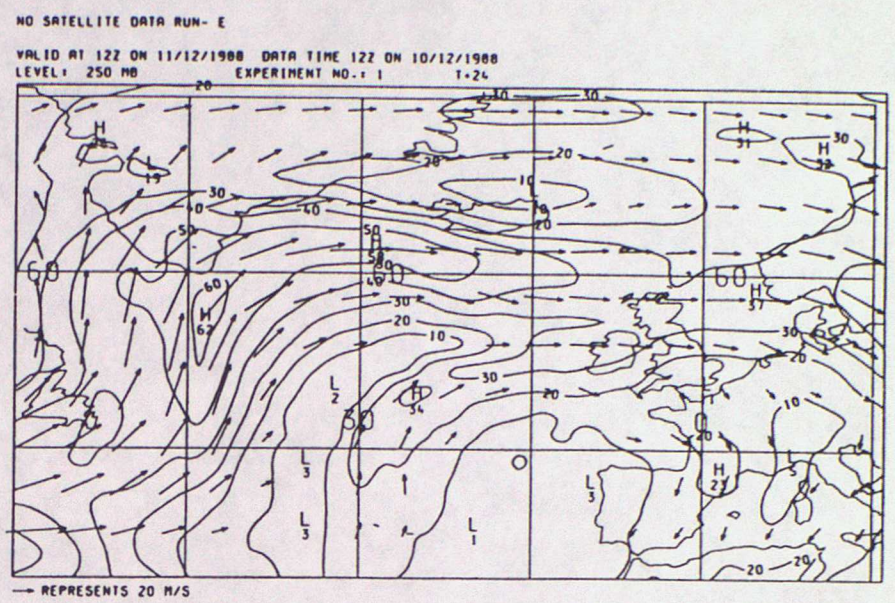

FIGURE 5. FINE-MESH 250MB WIND SPEED DIFFERENCES AT T+24, VALID 12Z 11/12/88

(iii) C-E

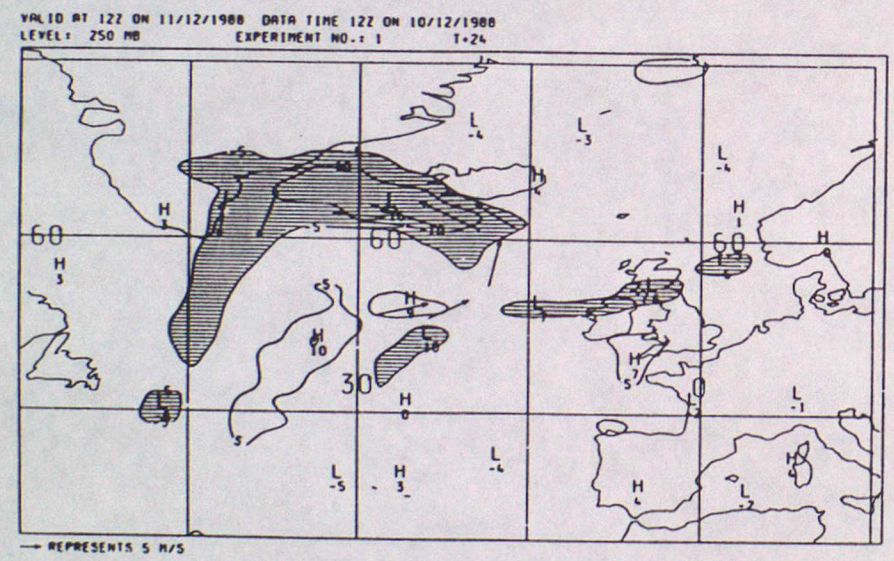

(iv) D-E

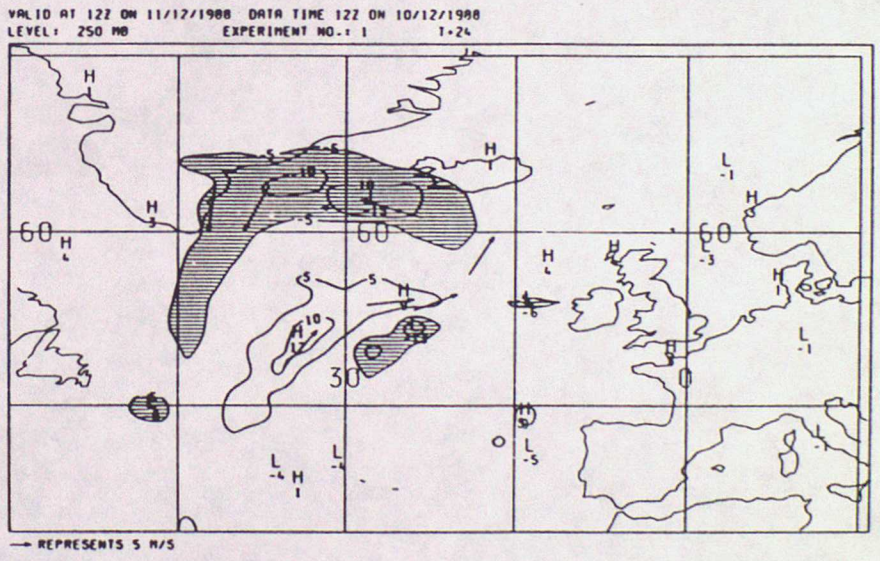

FIGURE 6. THICKNESS DIFFERENCE BETWEEN THE RETRIEVED 1000-500MB THICKNESS FROM SOUNDING DATA AND THE FINE-MESH FORECAST BACKGROUND THICKNESS

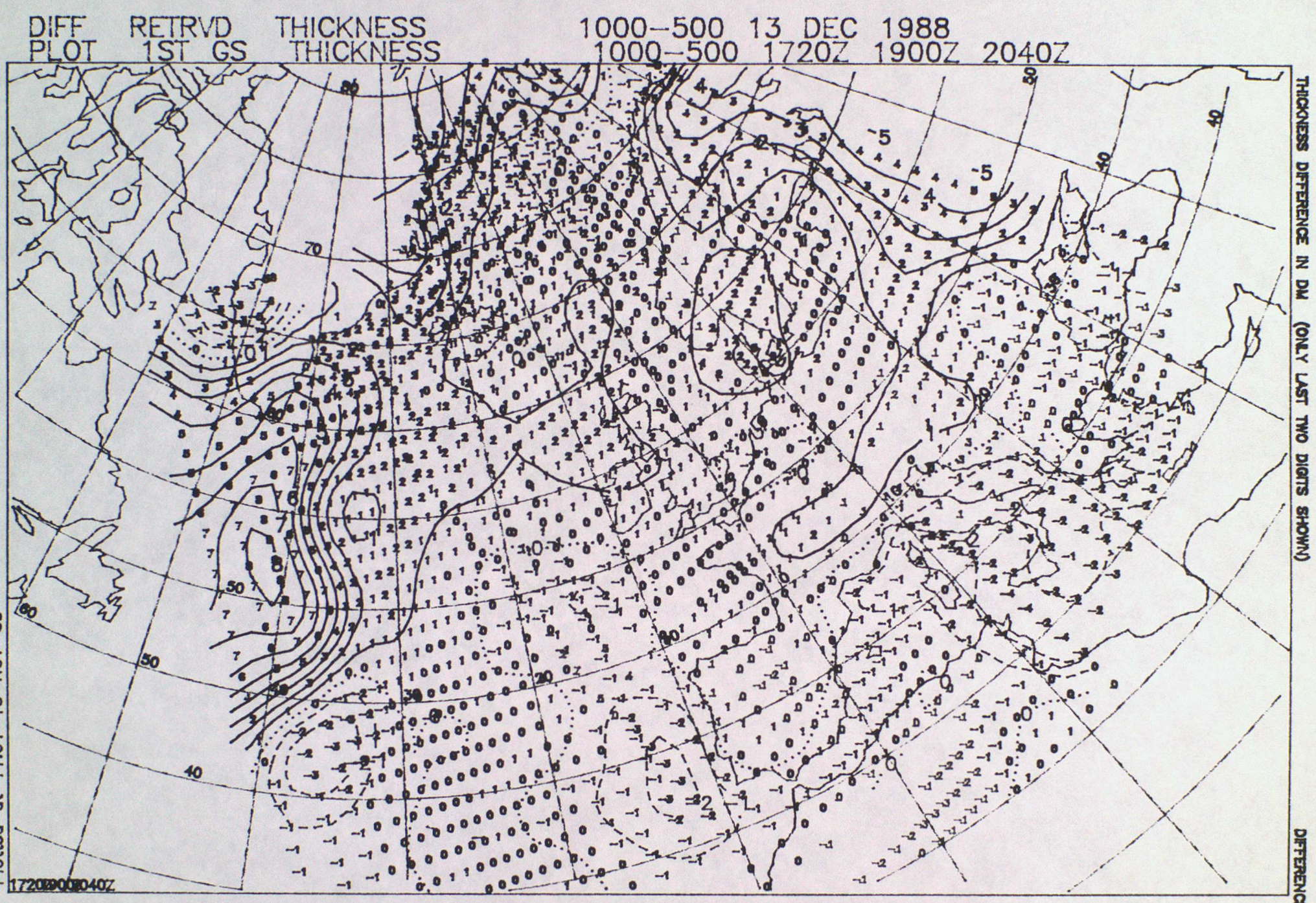

FIGURE 7. FINE-MESH 1000-500MB THICKNESS ANALYSIS AT 00Z 14/12/88

(i) FOLLOWING THE C ASSIMILATIONS (ii) FOLLOWING THE E ASSIMILATIONS

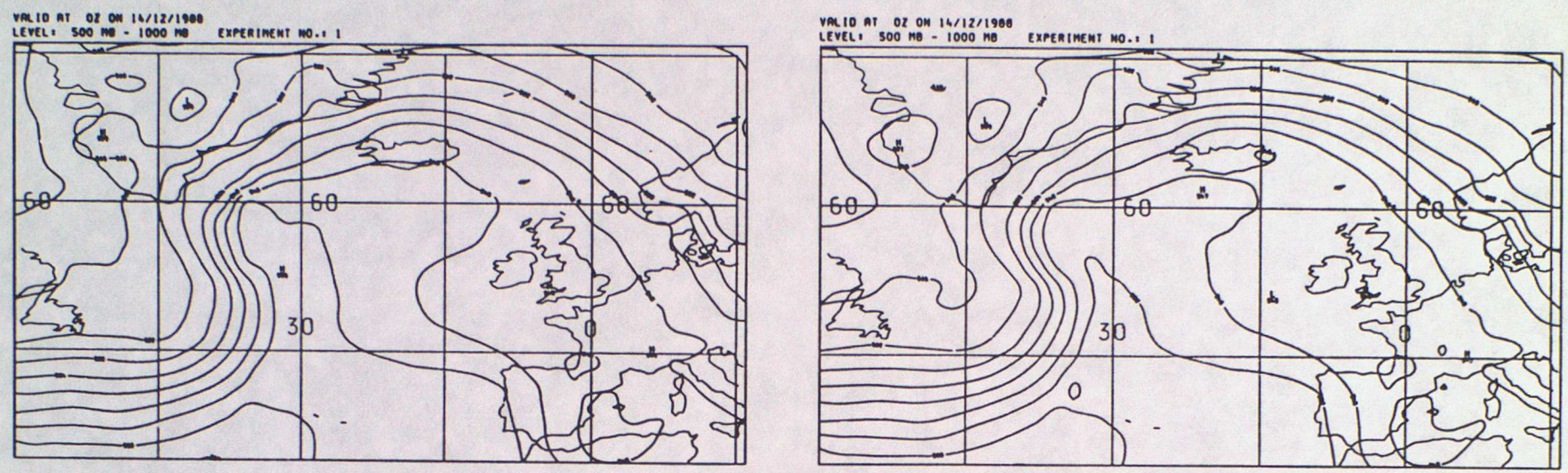

FIGURE 7. FINE-MESH 1000-500MB THICKNESS DIFFERENCE CHARTS FOR 00Z 14/12/88

(iii) C-E

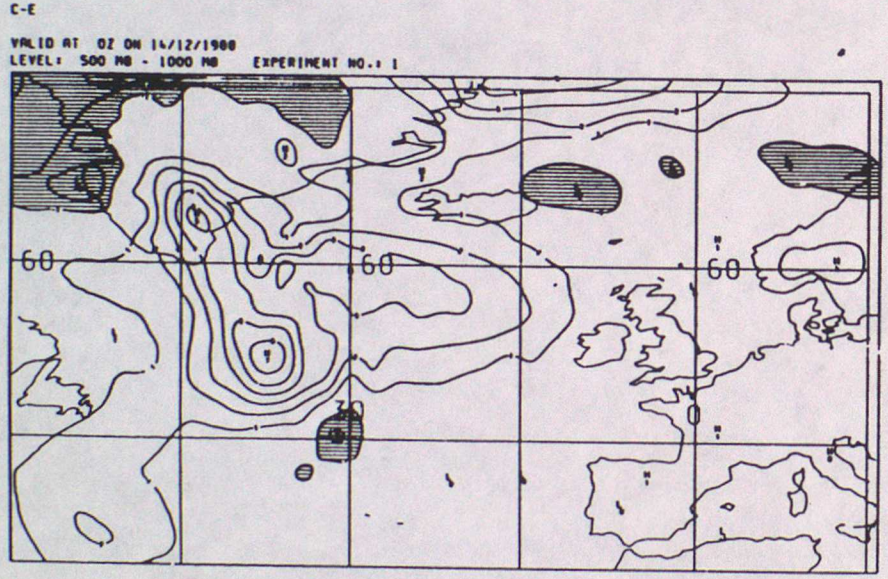

FIGURE 8. FINE-MESH 1000-500MB THICKNESS FORECAST AT T+12 VALID 12Z 14/12/88

(i) EXPERIMENT C

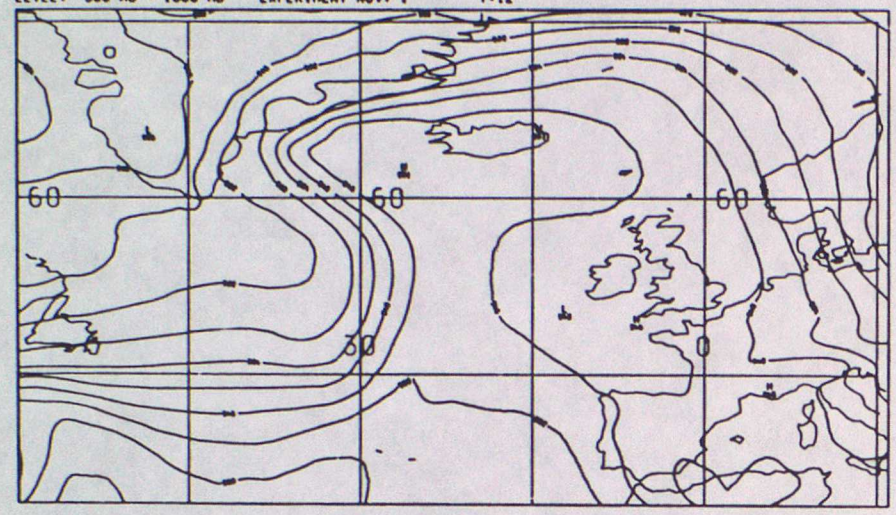

(ii) EXPERIMENT E

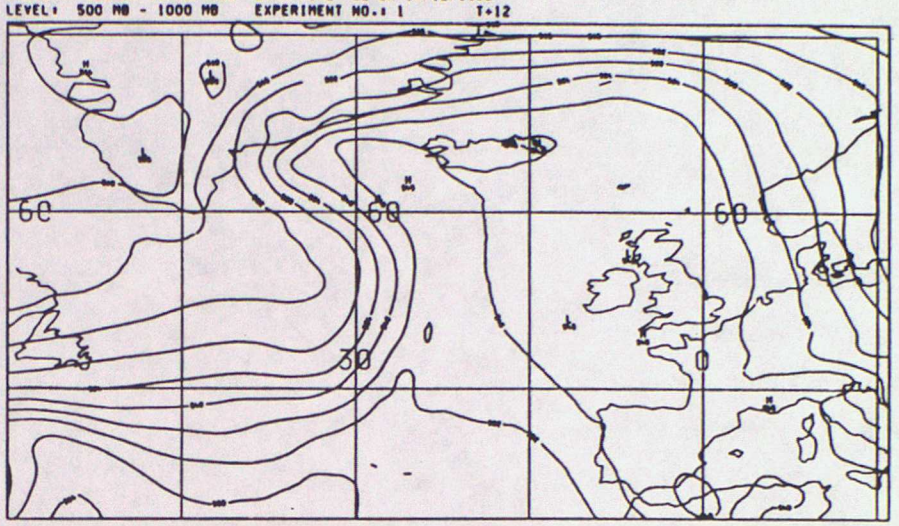

FIGURE 8. FINE-MESH 1000-500MB THICKNESS DIFFERENCE CHARTS FOR C-E

(iii) T+12 VALID 12Z 14/12/88

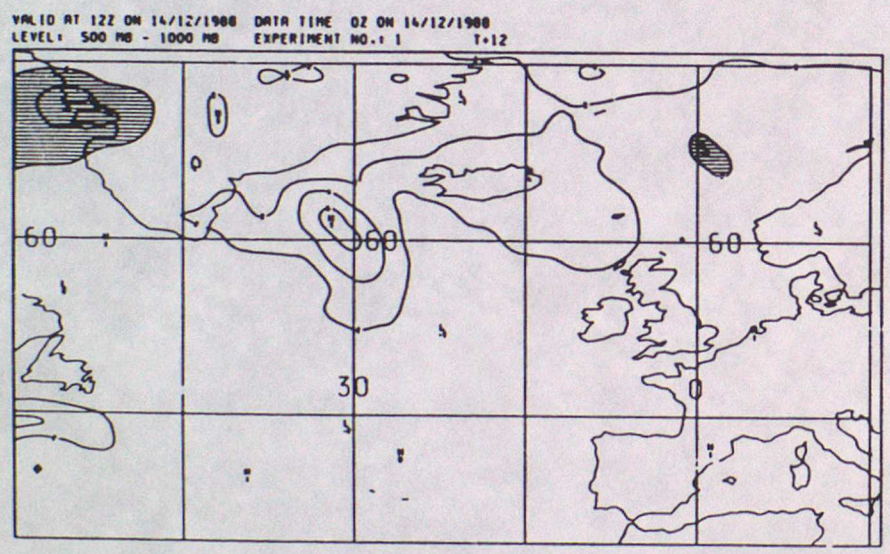

(iv) T+24 VALID 00Z 15/12/88

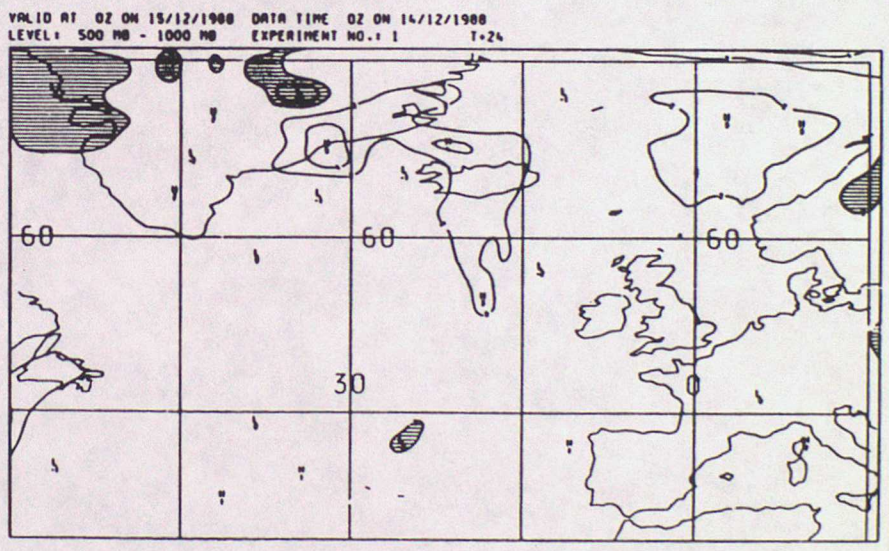

FIGURE 9 B-E 1000-500MB THICKNESS DIFFERENCE CHARTS

(i) ANALYSIS AT 00Z 14/12/88 (ii) T+12 FORECAST VALID 12Z 14/12/88

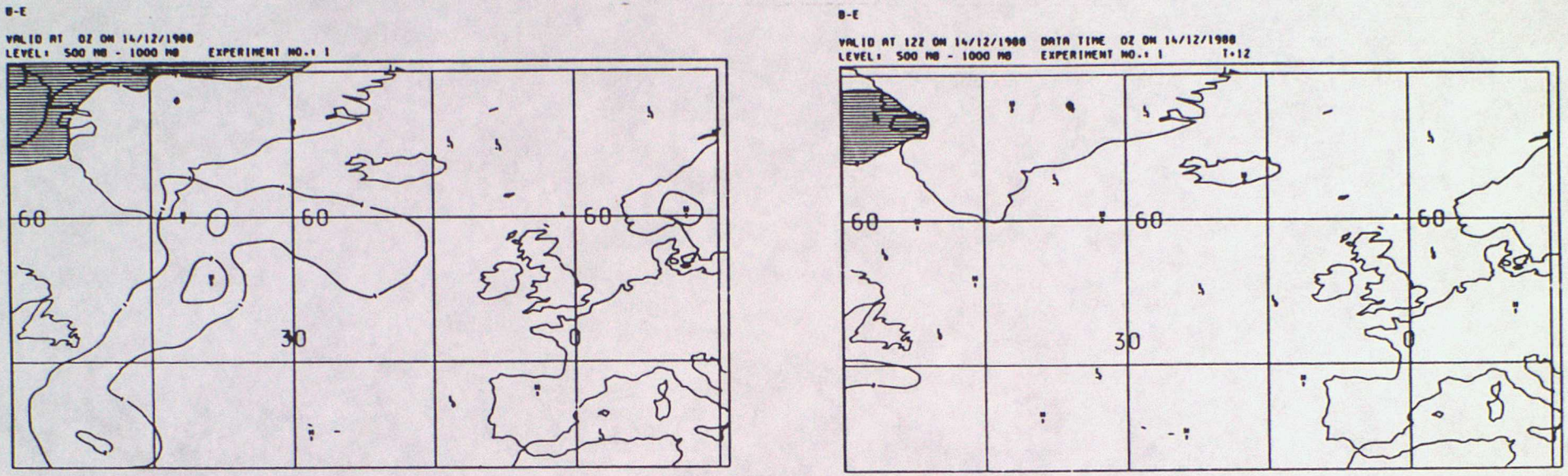

FIGURE 9 D-E 1000-500MB THICKNESS DIFFERENCE CHARTS

(iii) ANALYSIS AT 00Z 14/12/88 (iv) T+12 FORECAST VALID 12Z 14/12/88

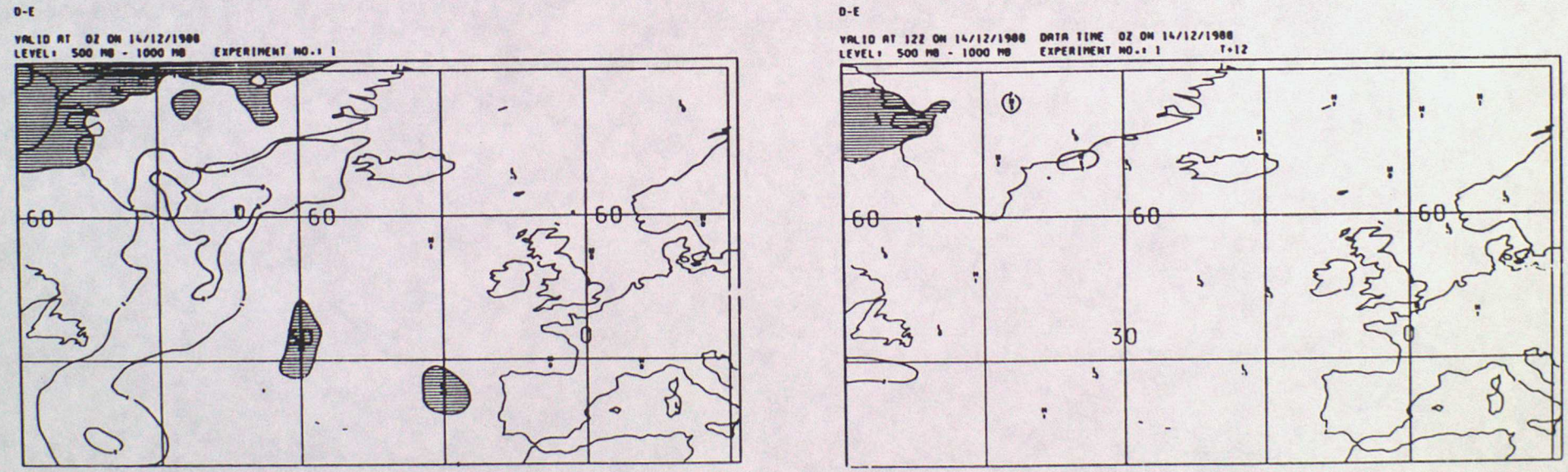

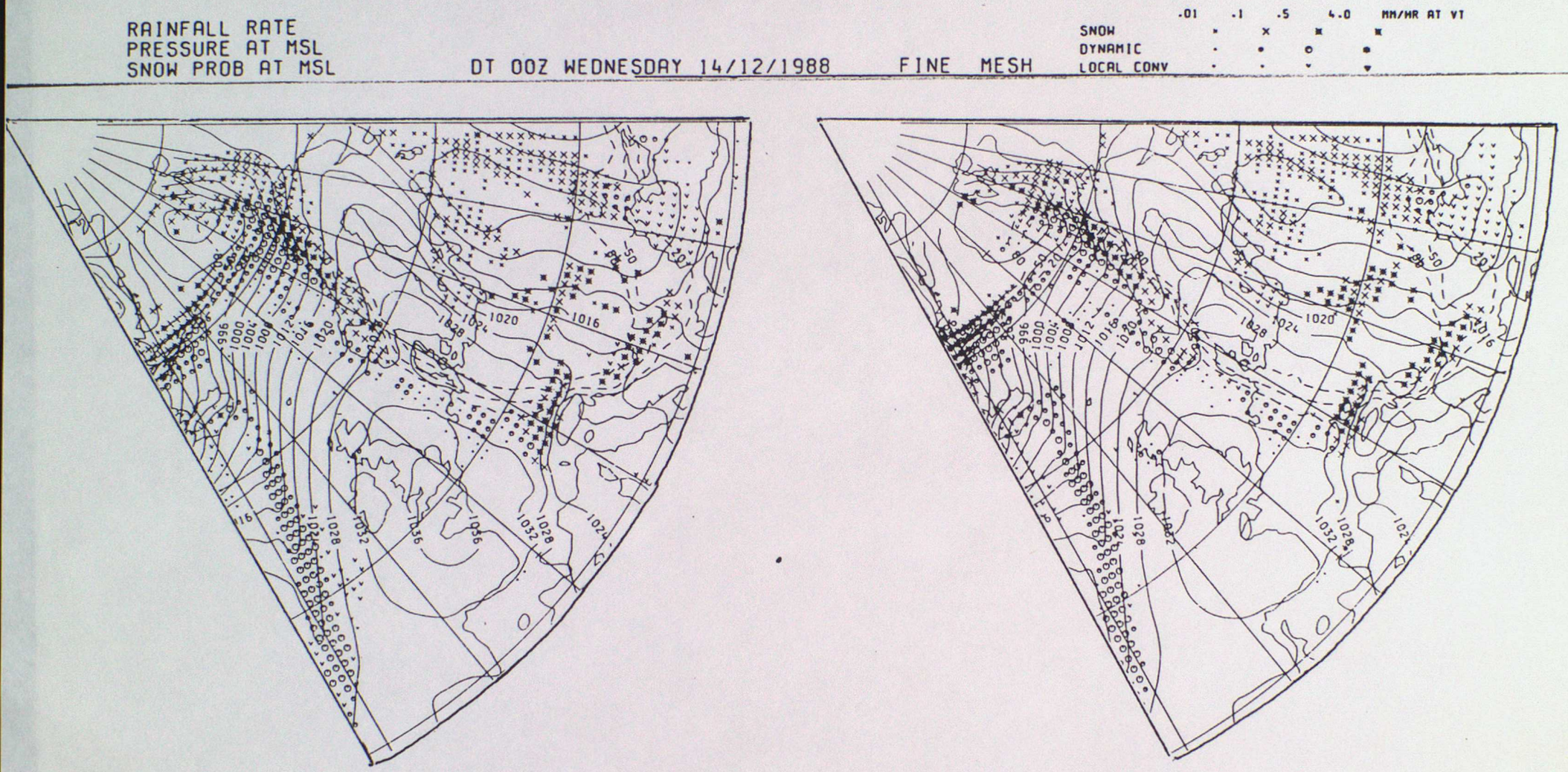

FIGURE 10 FINE-MESH MODEL T+24 FINE-MESH MODEL T+24 FORECASTS OF RAINFALL RATE AND MEAN SEA LEVAL PRESSURE VALID 00Z 15/12/88

(i) FORECAST C

(ii) FORECAST E

FIGURE 11 FINE-MESH 250MB WIND ANALYSIS VALID 00Z 14/12/88

(i) FOLLOWING THE C ASSIMILATIONS

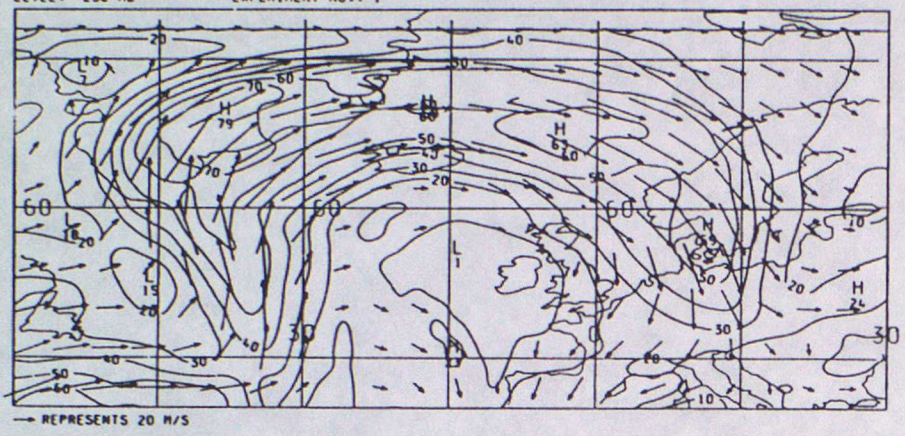

(ii) FOLLOWING THE E ASSIMILATIONS

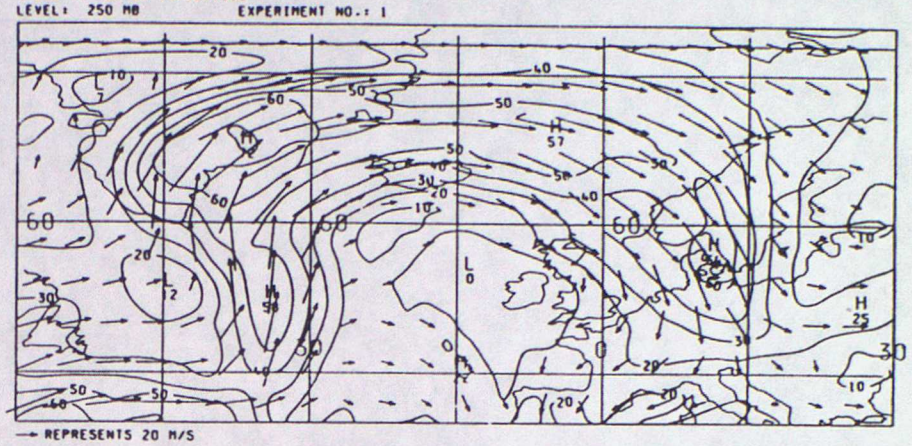

FIGURE 11 FINE-MESH 250MB WIND ANALYSIS DIFFERENCES VALID 00Z 14/12/88

(iii) C-E

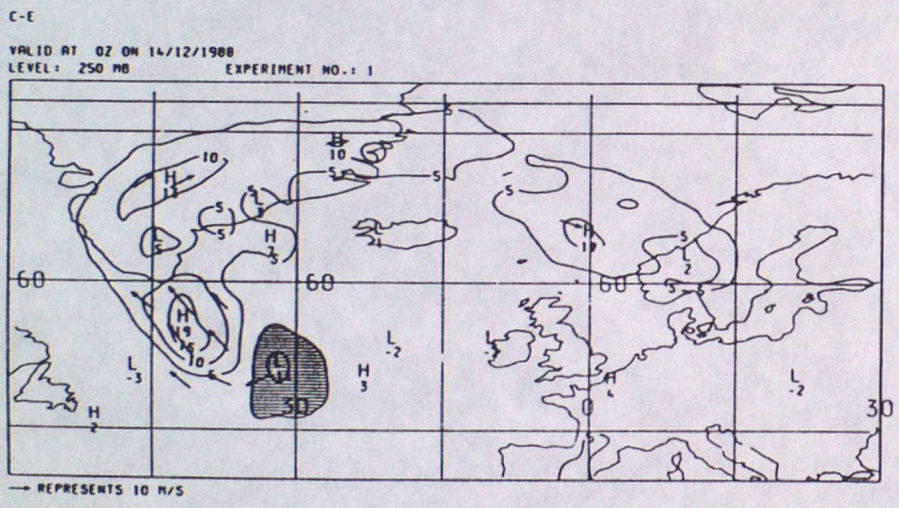

FIGURE 12 THICKNESS DIFFERENCE BETWEEN THE RETRIEVED 1000-500MB THICKNESS FROM SOUNDING DATA AND THE FINE-MESH FORECAST BACKGROUND THICKNESS

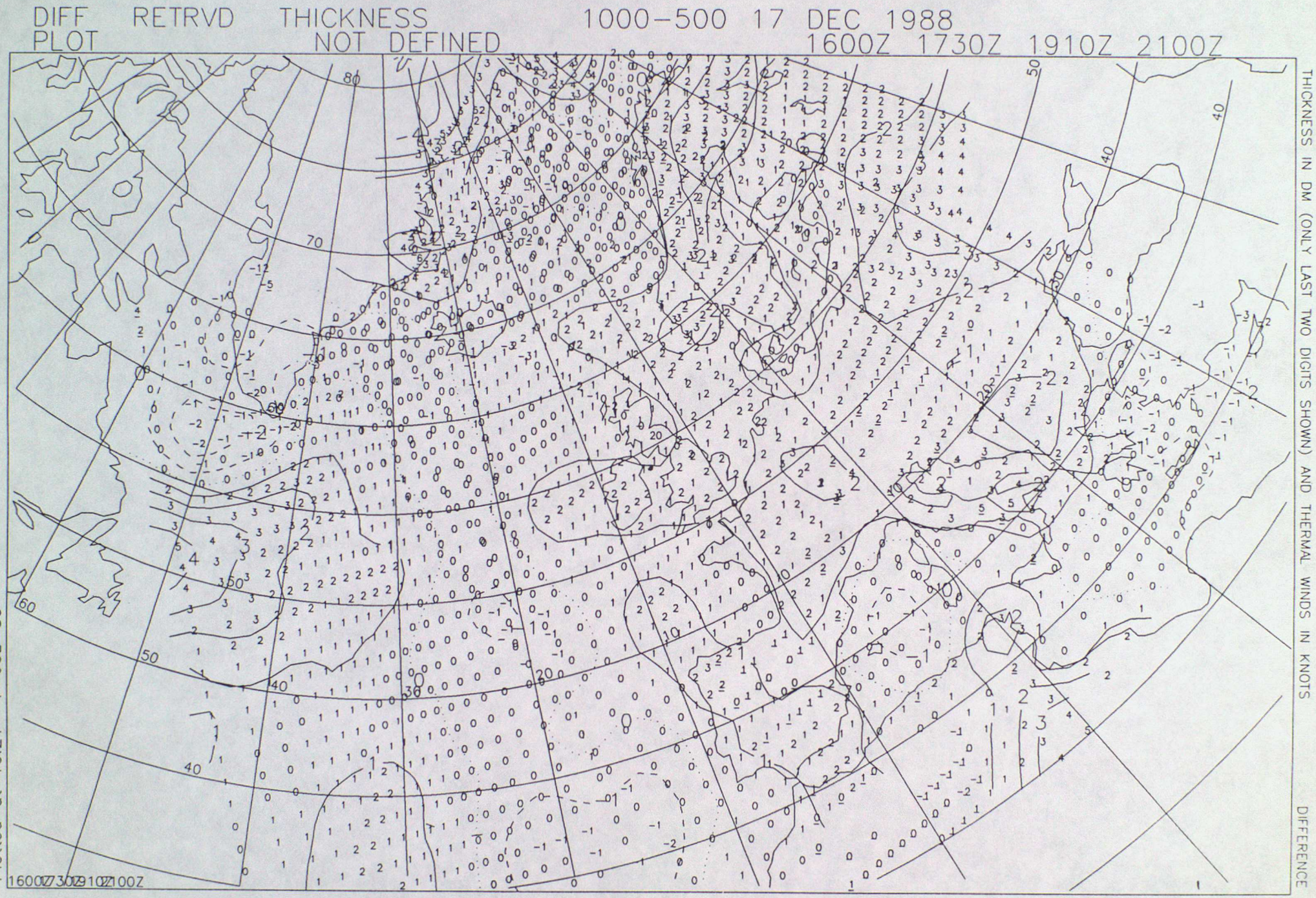

(i) FOLLOWING THE C ASSIMILATIONS (ii)FOLLOWING THE E ASSIMILATIONS

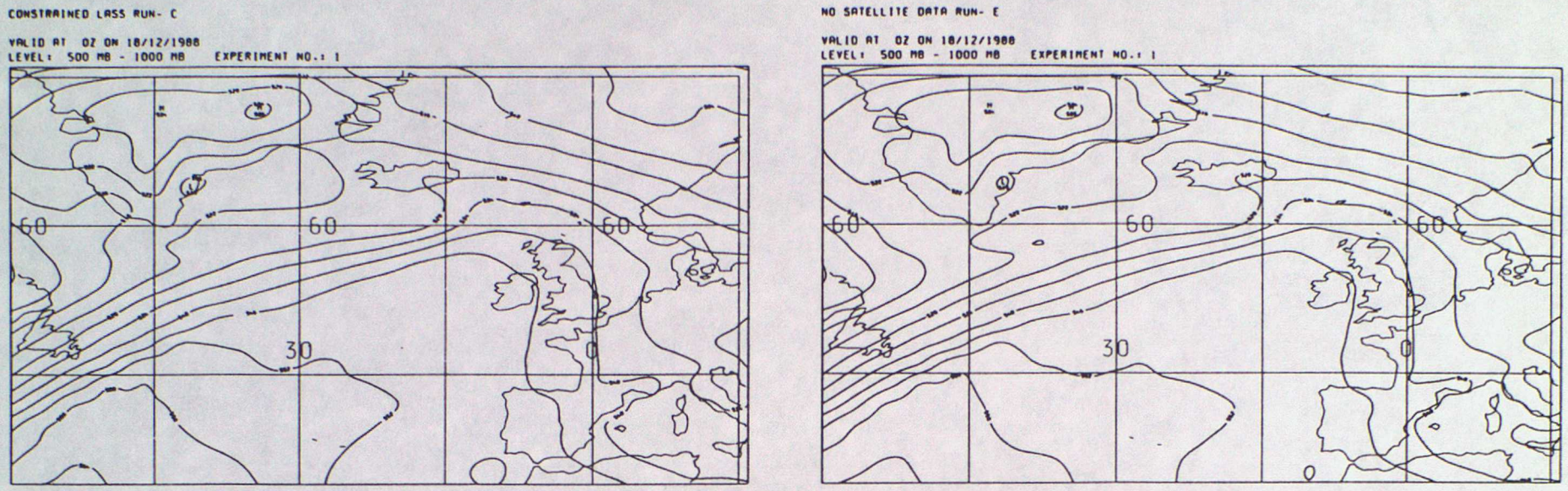

FIGURE 13 FINE-MESH 1000-500MB THICKNESS DIFFERENCE CHARTS

(iii) C-E ANALYSIS VALID 00Z 18/12/88 (iv)C-E T+24 FORECAST VALID 00Z 19/12/88

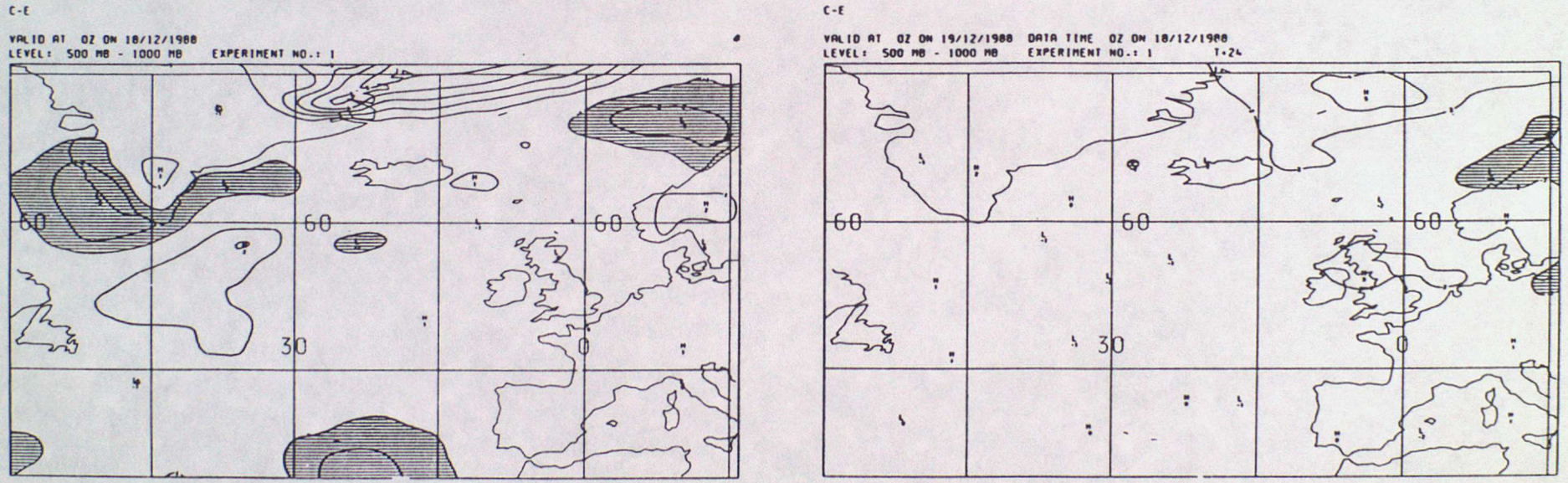

FIGURE 14 FINE-MESH T+24 FORECAST RAINFALL RATES AND MEAN SEA LEVEL PRESSURE PLUS THE OBSERVED RAIN AREA ALL VALID 00Z 19/12/88

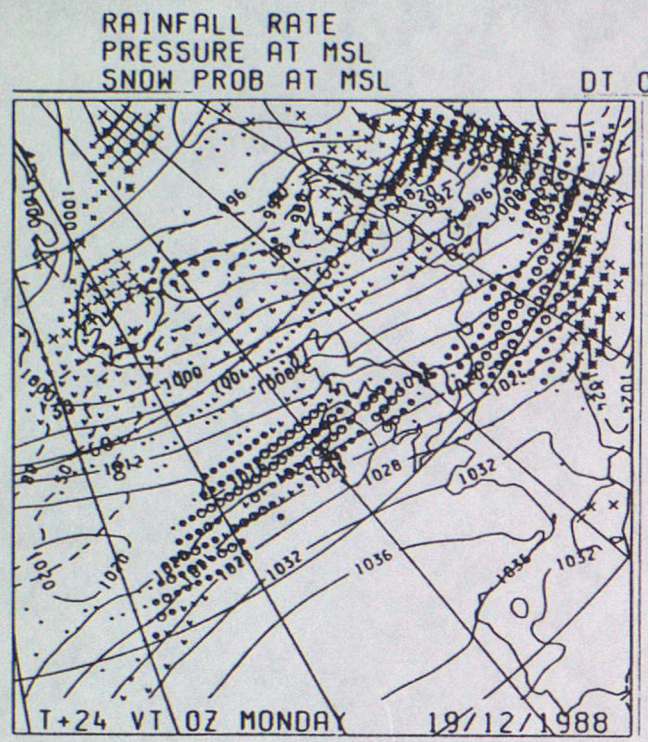

(i) FORECAST C

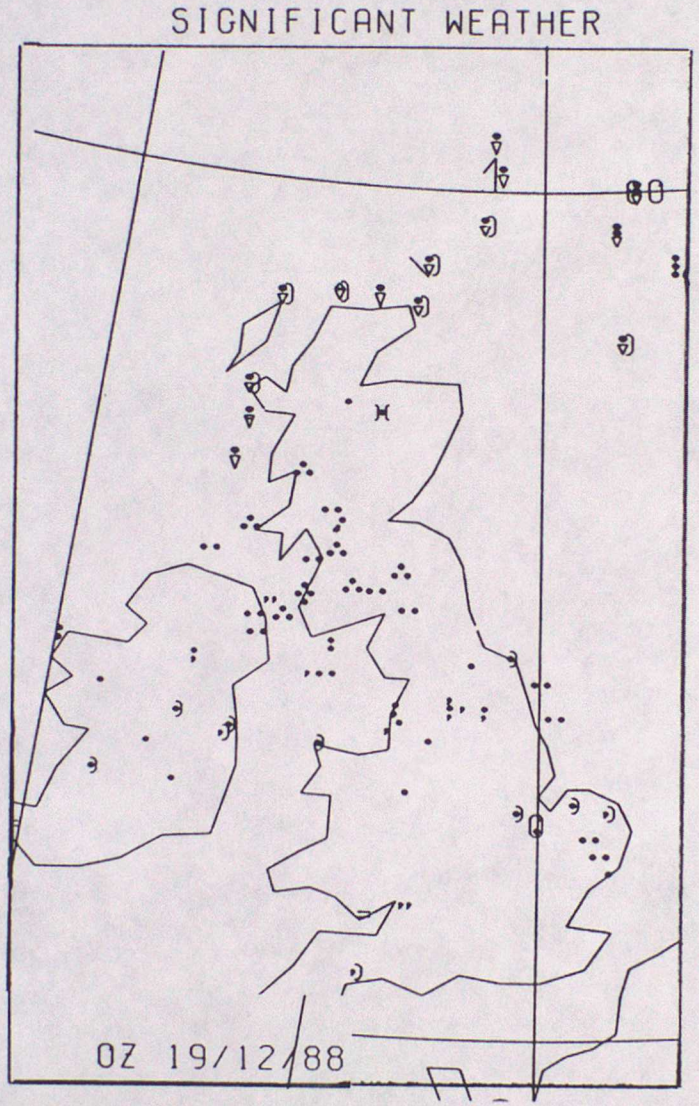

(iii) OBSERVED RAIN AREA

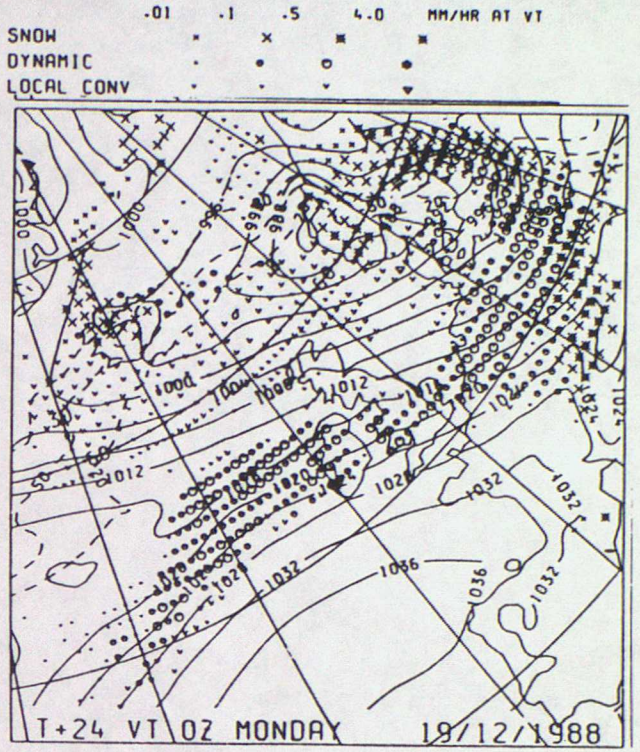

(ii) FORECAST E

FIGURE 15 FINE-MESH MODEL 250MB WIND ANALYSIS VALID AT 12Z 19/12/88

(i) FOLLOWING THE C ASSIMILATIONS

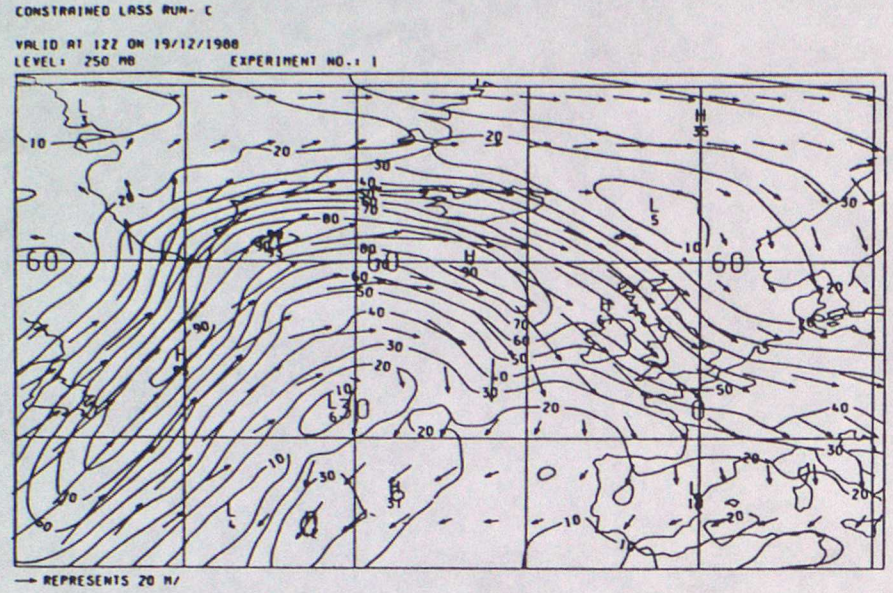

(ii) FOLLOWING THE E ASSIMILATIONS

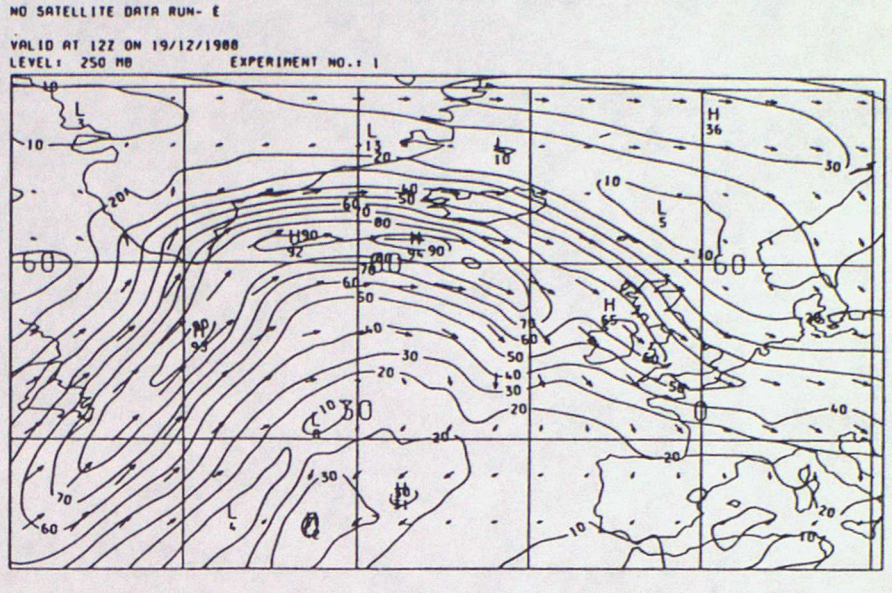

FIGURE 15 FINE-MESH MODEL 250MB WIND SPEED ANALYSIS DIFFERENCES AT 12Z 19/12/88

(iii) C-E

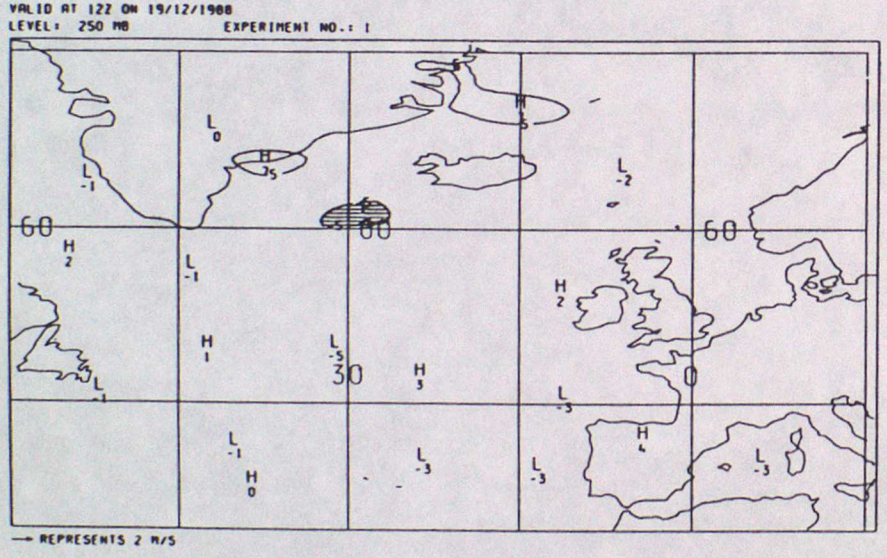

FIGURE 16 FINE-MESH MODEL 250MB WIND T+12 FORECAST VALID AT 00Z 20/12/88

(i) FORECAST C (SPEED IN M/S)

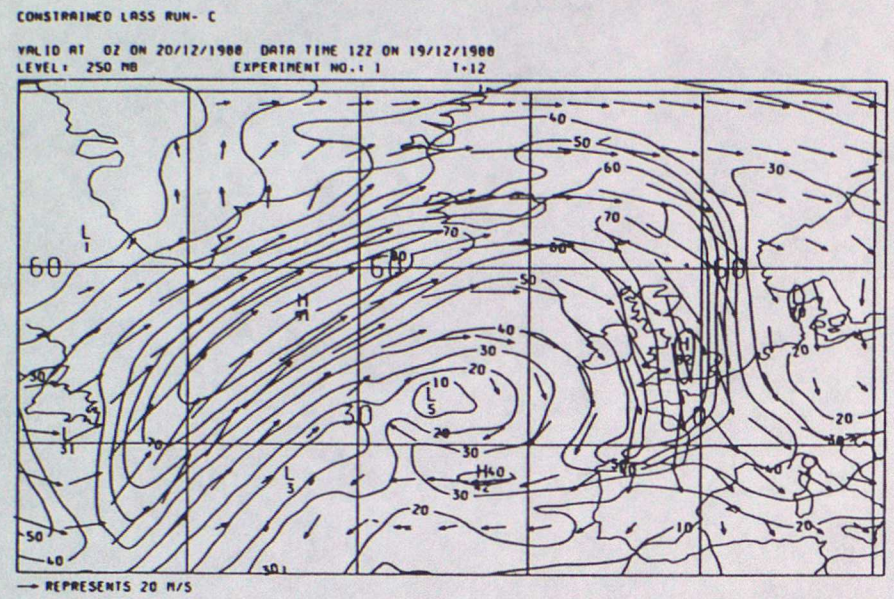

(ii) FORECAST E (SPEED IN M/S)

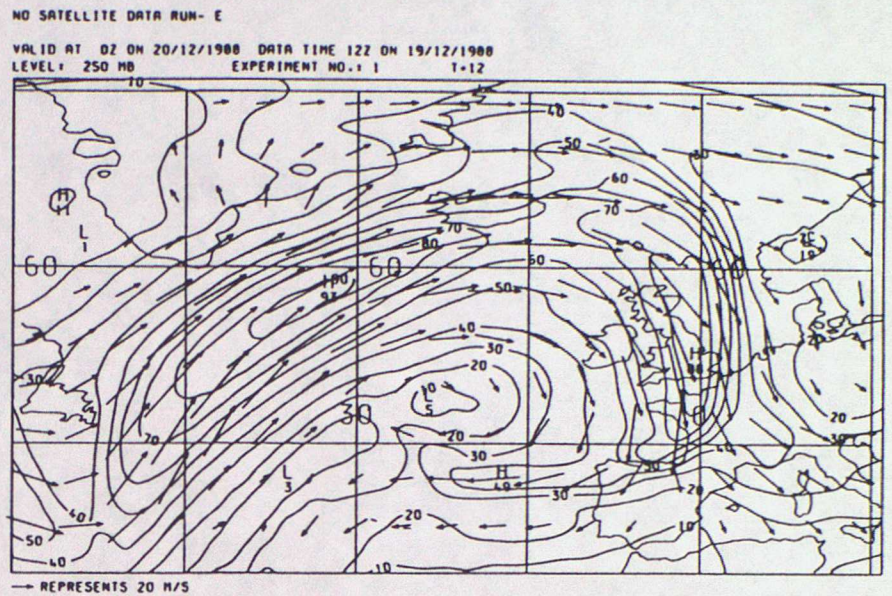

FIGURE 16 FINE-MESH MODEL 250MB WIND SPEED FORECAST DIFFERENCES AT 12Z 19/12/88

(iii) C-E T+12

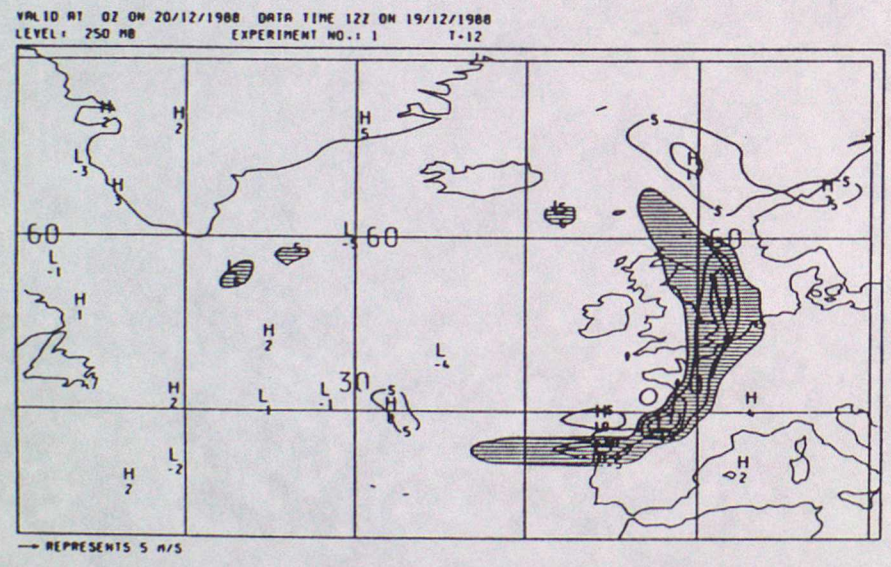

FIGURE 16 (iv)WIND SPEED IN KNOTS

OBSERVATIONS FOR 00Z ON 20/12/1988 LEVEL= 250 MB

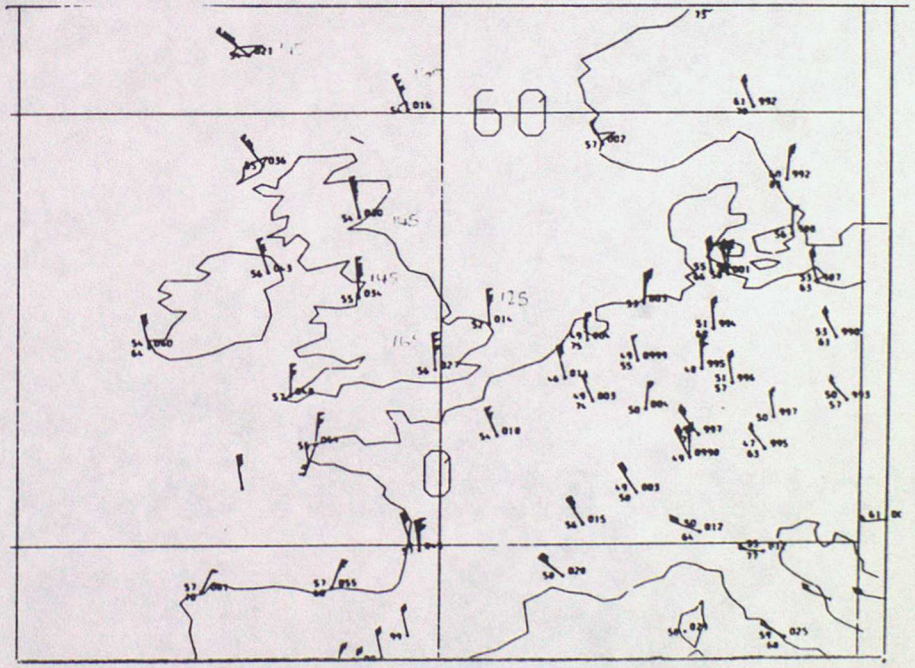

F[redacted]E [redacted]FIN[redacted]SH [redacted]8 [redacted]CAS[redacted]AIN[redacted]. R[redacted]S A[redacted]ME[redacted]SEA[redacted]VEL

PRESSURE PLUS THE OBSERVED RAIN AREA ASSOCIATED WITH WARM FRONT VALID 06Z

20/12/88

RAINFALL RATE
PRESSURE AT MSL
SNOW PROB AT MSL

DT 12Z MONDAY 19/12/1988 FINE MESH

	.01	.1	.5	4.0	MM/HR AT VT
SNOW	·	×	✱	✱	
DYNAMIC	·	•	o	●	
LOCAL CONV	·	·	˅	▼	

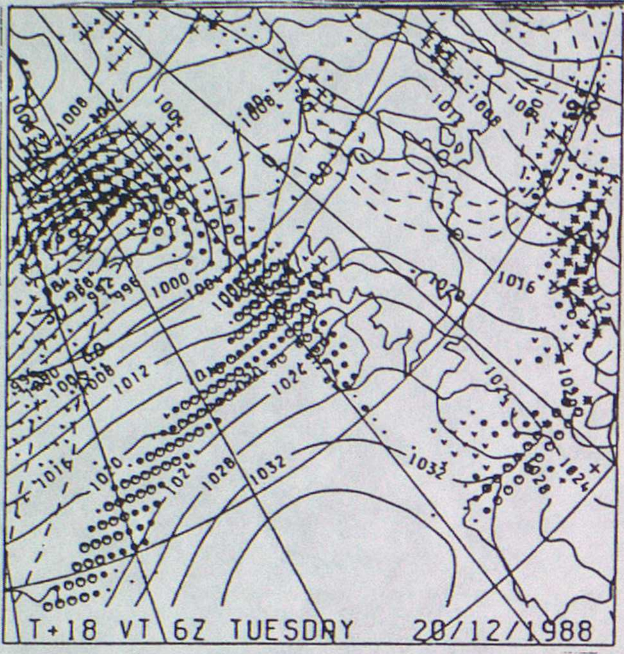

(i) FORECAST C

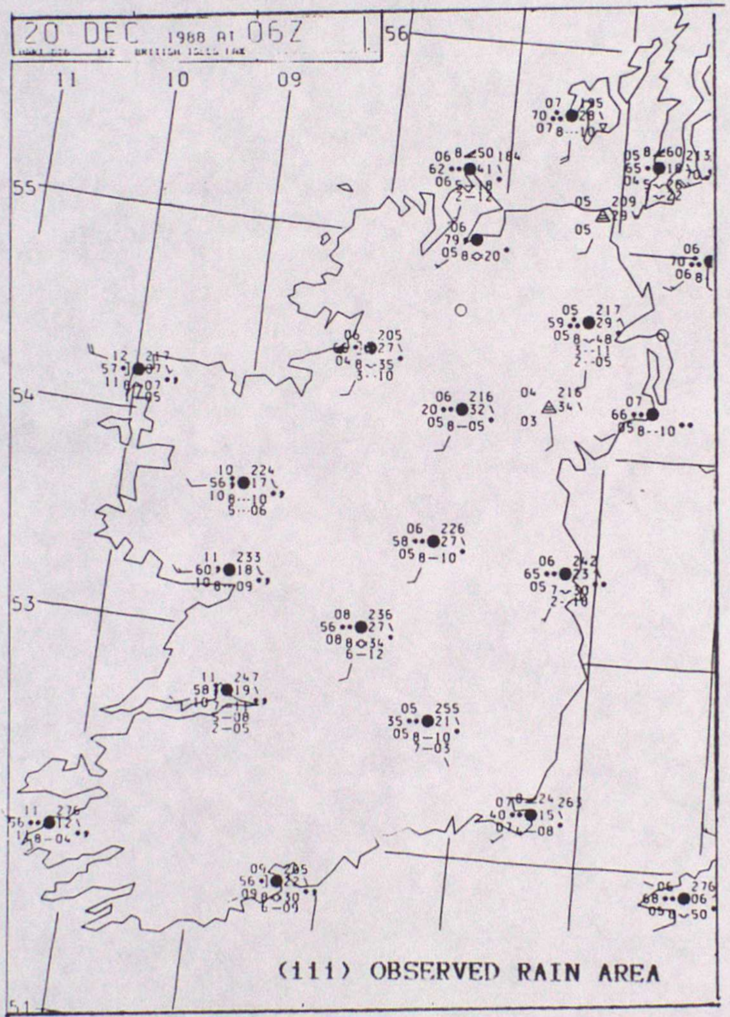

(iii) OBSERVED RAIN AREA

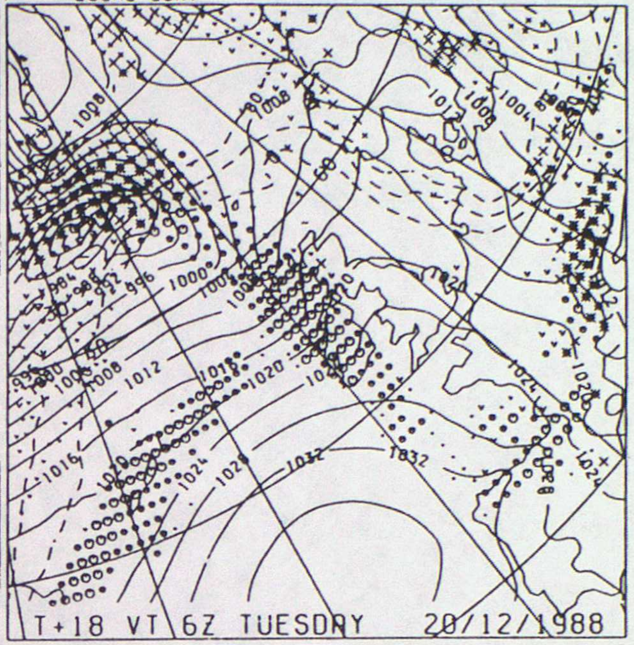

(ii) FORECAST E

CURRENT MET O 11 TECHNICAL NOTES (JANUARY 1989)

The Met O 11 Technical Notes which contain information of current use and *which have not been published* elsewhere, are listed below. The complete set of Technical Notes is available from the National Meteorological Library on loan, if required.

186. The representation of boundary layer turbulence in the mesoscale model. Part 1. The scheme without changes of state.
R.N.B. Smith
April 1984

187. The representation of boundary layer turbulence in the mesoscale model. Part 2. The scheme with changes of state.
R.N.B. Smith
April 1984

195. Assessment of HERMES data: a case study comparison with the operational analysis for 2nd March 1984.
W. Adams
August 1984

196. Solutions in flow over topography using a geometric Lagrangian flow.
S. Chynoweth
November 1984

197. An investigation into the likely causes of spurious rain in anticyclones in the fine mesh model.
W. Hand
October 1984

199. The impact of data from the HERMES system on the fine mesh data assimilation scheme - a case study.
R.S. Bell and O.M. Hammon
February 1985

203. Using an interactive radiation scheme in the fine mesh model.
A.D. Darlington
March 1985

204. Snow forecasts from NWP models during the winter of 1984/85.
O.M. Hammon
March 1985

205. Results of a trial of a parametrization of gravity wave drag in the operational forecast model.
J.E. Kitchen, M.J. Carter and A.P. Day
April 1985

206. **Parametrization of viscosity in three dimensional vortex methods and finite difference models.**
S.P. Ballard
April 1985

207. **A mesoscale simulation of the cold front of 12.11.84.**
B.W. Golding
October 1985

208. **Subgrid-scale cloudiness in the UKMO mesoscale model.**
N. Machin
May 1985

209. **An examination of the structure of fronts in the Met. Office and ECMWF models.**
W. Hand
August 1985

211. **Solutions of a Lagrangian conservation law model of atmospheric motions**
M.J.P. Cullen, J. Norbury and R.J. Purser
August 1985

212. **The analysis of high resolution satellite data in the Met Office.**
A.C. Lorenc, W. Adams and J. Eyre
August 1985

215. **A shortcoming of the operational convection scheme at higher resolution**
M.W. Holt
September 1985

219. **Three dimensional vortex methods and their application to the direct simulation of turbulence.**
S.P. Ballard
October 1985

222. **An implicit version of the operational model boundary layer routine.**
J.E. Kitchen
1986

224. **Four-dimensional analysis by repeated insertion of observations into a NWP model.**
A.C. Lorenc and R. Dumelow
December 1985, revised July 1987

226. **A study of the structure of mid-latitude depressions in a numerical model using trajectory techniques, II. Case studies.**
B.W. Golding
1986

228. **Investigation of balance in the operational global model with normal mode initialization.**
B. Macpherson
April 1986

229. **A parametrization of deep convection for use in a non-hydrostatic mesoscale model.**
R.T.H. Barnes and B.W. Golding
March 1986

230. **Boundary layer structures and surface variables in operational forecasts.**
R.S. Bell
April 1986

231. **Meteorological Office mesoscale model: an overview, version 1.**
B.W. Golding
December 1986

235. **Snow forecasts from the fine mesh model and mesoscale model during the winter 1985/86.**
O.M. Hammon
June 1986

236. **Vertically-propagating quasi-inertia waves: simulated and observed.**
M.M. Booth and G.J. Shutts
November 1986

239. **Mesoscale case study - Project Haar.**
W.R.P. Taylor
February 1987

240. **A trial of modified diffusion in the coarse mesh model.**
R.S. Bell and R.A. Downton
September 1986

243. **The global impact of the recent developments of the physical parameterisation schemes.**
R.S. Bell
November 1986

247. **Some experiments with two-dimensional semi-geostrophic and primitive equation models, with sigma as the vertical coordinate.**
C.A. Parrett
February 1987

248. **Moist frontogenesis in the geometric model.**
M.W. Holt
March 1987

249. **Mesoscale model trial of a revised convection scheme and cloud modifications.**
O.M. Hammon
May 1987

250. **Results from the fine mesh trial of a modified physics package.**
O.M. Hammon
July 1987

251. **Verification of mesoscale model forecasts during the winter, November 1986 - February 1987.**
O.M. Hammon
March 1987

252. **Mountain wave generation by models of flow over synoptic-scale orography.**
M.J.P. Cullen and C.A. Parrett
March 1987

253. **Development of the analysis correction scheme, I. The observational weights.**
B. Macpherson
September 1987

256. **Experiments with divergence damping and reduced diffusion in the mesoscale model.**
S.P. Ballard
May 1987

258. **Trials of the interactive radiation scheme in the global model.**
M.D. Gange
May 1987

261. **Modifications to the automatic quality control of ship data and an assessment using case studies.**
B.R. Barwell and C.A. Parrett
1987

263. **Results from a fine mesh model trial using a modified evaporation scheme.**
O.M. Hammon and C.A. Wilson
August 1987

NEW SERIES (Commenced October 1987)

1. **An assessment of the results of trials of a new analysis scheme for the operational global model.**
R.S. Bell
October 1987

2. **A case study showing the impact of analysis differences on medium range forecasts.**
R.A. Downton and R.S. Bell
January 1988

3. **Development of the analysis correction scheme. II. Inclusion of an observation density analysis.**
B. Macpherson
September 1988

4. **An assessment of a trial to test small changes to the Convection scheme in the mesoscale model.**
O.M. Hammon
January 1988

5. **Trial of proposed changes to the Mesoscale model for November 1987.**
O.M. Hammon
December 1987

6. **Assessment of HERMES soundings processed using the new cloud-clearing scheme.**
R. Swinbank
March 1988

7. **An assessment of the impact of a correction to the Mesoscale model turbulence/vertical diffusion scheme implemented in March 1988.**
S.P. Ballard and O.M. Hammon
April 1988

8. **Comparison of algorithms for the solution of cyclic, block, tridiagonal systems.**
M.H. Mawson
May 1988

9. **A comparison of alternating direction implicit methods for solving the 3-D semi-geostrophic equations.**
M.H. Mawson
May 1988

10. **The automatic quality control of surface observations from ships: the final trial, latest statistics, operational implementation and future work.**
C.A. Parrett
May 1988

11. **"Panel-beater": a proposed fast algorithm for semi-geostrophic finite-element codes.**
R.J. Purser
June 1988

12. **The 5-day forecast trial of the AC scheme.**
R.A. Downton, R.A. Bromley and M.A. Ayles
September 1988

13. **A theoretical study of the information content of the ERS-1 scatterometer data.**
R.J. Purser
August 1988

14. **A further global trial of the analysis correction scheme - Christmas 1987.**
R.S. Bell
August 1988

15. **The sensitivity of a medium range forecast with the analysis correction scheme to data selection in the horizontal.**
B. Macpherson and R.A. Downton
Not yet issued.

16. **The sensitivity of fine-mesh rainfall forecasts to changes in the initial moisture fields.**
R.S. Bell and O.M. Hammon
August 1988

17. **Conservative finite difference schemes for a unified forecast/climate model.**
M.J.P. Cullen and T. Davies
July 1988

18. **Interpreting results from numerical models.**
T. Davies
August 1988

19. **A comparison of the OWSE assimilation scheme with the operational global assimilation scheme.**
D.N. Reed and M.A. Ayles
October 1988

20. **Improvements to low cloud forecasts from the mesoscale and fine mesh models.**
O.M. Hammon
October 1988

21. **The effect of route choice on aircraft wind observations over the North Atlantic.**
D. Lang and N.B. Ingleby
October 1988

22. **Maximum liklihood de-aliasing of simulated scatterometer wind fields using adaptive descent algorithms.**
R.J. Purser
January 1989

23. **A proposal for assimilating detailed aircraft wind data in a local area.**
R.J. Purser
January 1989

24. **Basic formulation and boundary conditions of the mesoscale model.**
S.P. Ballard
Not yet issued.

25. **Development of a new physics package for the global forecast model.**
C.A. Wilson and J. Slingo
January 1989

Recent Met O 11 Technical Notes (New Series)

26.	The trial of the fine-mesh version of the analysis correction scheme	O.M. Hammon R.A. Bromley B. Macpherson May 1989
27.	The New Meteorological Office Data Assimilation Scheme	A.C. Lorenc R.S. Bell B. Macpherson April 1989
28.	Model error structure and estimated analysis accuracy with a network of wind profilers	N.B. Ingleby R.A. Bromley April 1989
29.	Examples of hybrid vertical co-ordinate systems for the unified forecast/climate model.	R. Swinbank July 1989
30.	The Meteorological Office Experimental Mesoscale Numerical Weather Prediction System: July 1989	B.W. Golding July 1989
31.	Tests of the Heun Advection Scheme.	B.L. Marshall July 1989
32.	Not Yet Available	R.A. Bromley R.A. Downton
33.	Spatial diagnostics of operational assimiliations using the observation processing database.	P. Jemmer August 1989
34.	Enhancements to the Mesoscale Model and their impact on forecasts.	S.P. Ballard September 1989
35.	Preliminary stratospheric analysis experiments with the Analysis Correction scheme.	R. Swinbank October 1989
36.	A diagnostic study of the impact of Seasat scatterometer winds on numerical weather prediction.	N.B. Ingleby R.A. Bromley October 1989
37.	Extension of the Bayesian Ship Quality Control Scheme to all Surface Data, and a trial of the Quality Control of Land Synops.	C.A. Parrett O.M. Hammon November 1989
38.	The impact of satellite sounding data in the fine-mesh model.	R.S. Bell O. M. Hammon December 1989